




Interdomain interactions dictate the function of the *Candida albicans* Hsp110 protein Msi3

Received for publication, June 1, 2021, and in revised form, July 29, 2021. Published, Papers in Press, August 14, 2021.
<https://doi.org/10.1016/j.jbc.2021.101082>

Hongtao Li¹, Liqing Hu^{1,2} , Crist William Cuffee¹, Mahetab Mohamed¹, Qianbin Li², Qingdai Liu³, Lei Zhou¹, and Qinglian Liu^{1,*}

From the ¹Department of Physiology and Biophysics, Virginia Commonwealth University, Richmond, Virginia, USA; ²Department of Medicinal Chemistry, Xiangya School of Pharmaceutical Sciences, Central South University, Changsha, Hunan, China; and ³Key Laboratory of Food Nutrition and Safety, Tianjin University of Science & Technology, Tianjin, China

Edited by Ursula Jakob

Heat shock proteins of 110 kDa (Hsp110s), a unique class of molecular chaperones, are essential for maintaining protein homeostasis. Hsp110s exhibit a strong chaperone activity preventing protein aggregation (the “holdase” activity) and also function as the major nucleotide-exchange factor (NEF) for Hsp70 chaperones. Hsp110s contain two functional domains: a nucleotide-binding domain (NBD) and substrate-binding domain (SBD). ATP binding is essential for Hsp110 function and results in close contacts between the NBD and SBD. However, the molecular mechanism of this ATP-induced allosteric coupling remains poorly defined. In this study, we carried out biochemical analysis on Msi3, the sole Hsp110 in *Candida albicans*, to dissect the unique allosteric coupling of Hsp110s using three mutations affecting the domain–domain interface. All the mutations abolished both the *in vivo* and *in vitro* functions of Msi3. While the ATP-bound state was disrupted in all mutants, only mutation of the NBD-SBD β interfaces showed significant ATPase activity, suggesting that the full-length Hsp110s have an ATPase that is mainly suppressed by NBD-SBD β contacts. Moreover, the high-affinity ATP-binding unexpectedly appears to require these NBD-SBD contacts. Remarkably, the “holdase” activity was largely intact for all mutants tested while NEF activity was mostly compromised, although both activities strictly depended on the ATP-bound state, indicating different requirements for these two activities. Stable peptide substrate binding to Msi3 led to dissociation of the NBD-SBD contacts and compromised interactions with Hsp70. Taken together, our data demonstrate that the exceptionally strong NBD-SBD contacts in Hsp110s dictate the unique allosteric coupling and biochemical activities.

Heat shock proteins of 110 kDa (Hsp110s) form a unique class of molecular chaperones (1–9). Ubiquitously present in the eukaryotic cytosol, they play an essential role in maintaining cellular protein homeostasis. Through this role, they provide essential protections for eukaryotic organisms against various stress conditions, including many human diseases. Thus, it is paramount to characterize the precise mechanism(s)

of their action in maintaining protein homeostasis to understand their protective role against various diseases.

As distant homologs of Hsp70s, Hsp110s are both chaperones on their own and cochaperones for Hsp70s. Hsp70s, an essential and universal class of molecular chaperones, play key roles in virtually all known processes in maintaining protein homeostasis (10–17). Hsp110s, by themselves, have potent chaperone activity in preventing the aggregation of denatured proteins, the “holdase” activity (18–21). However, they lack the hallmark activity of Hsp70s in assisting protein folding directly. As cochaperones, Hsp110s have been shown to function as the major nucleotide-exchange factors (NEFs) for cytosolic Hsp70s, facilitating the exchange of ADP for ATP in Hsp70s after ATP hydrolysis (3, 4, 9, 22, 23). Various studies have demonstrated that Hsp110s participate in almost all the processes that are associated with cytosolic Hsp70s including *de novo* protein folding and refolding under stress, protein transportation into the endoplasmic reticulum, solubilizing protein aggregates, and protein degradation (1, 5, 7–9, 18–20, 24–39). However, the functional roles of Hsp110s beyond NEFs remain a mystery.

The unique biochemical properties of Hsp110s dictate their special chaperone activities. As homologs, Hsp110s share the same domain organization as Hsp70s (1, 8, 9, 14, 40). Both Hsp110s and Hsp70s have two functional domains: a nucleotide-binding domain (NBD) at the N-terminus and a substrate-binding domain (SBD) at the C-terminus. The SBD is further divided into SBD β and SBD α . Connecting these two functional domains is a short interdomain linker. Hsp110s are larger in size due to an insertion in the SBD β and a C-terminal extension beyond the SBD α . A recent study suggested a novel substrate-binding site in the C-terminal extension region of metazoan Hsp110s but not yeast Hsp110s (41). However, it is puzzling that both these extra segments are dispensable for function (6, 40, 42).

The biochemical properties and structures of Hsp70s are well studied. For Hsp70s, each functional domain has an essential intrinsic activity (10, 11, 13, 14, 43, 44). The NBD binds ATP or ADP and hydrolyzes bound ATP to ADP, *i.e.*, the NBD has an ATPase activity. The SBD binds hydrophobic segments of polypeptides in extended conformation, normally only found in unfolded proteins. As there is little contact

* For correspondence: Qinglian Liu, qinglian.liu@vcuhealth.org.

The unique allosteric regulation of Hsp110

between the two domains in the ADP-bound and nucleotide-free (apo) states, the isolated SBD structures represent these states (45–47). In contrast, ATP binding allosterically couples the two functional domains (48, 49). This allosteric coupling is crucial for the chaperone activity by ensuring that the energy from ATP hydrolysis is efficiently used for regulating peptide substrate binding (14, 43, 45, 46, 48–55).

In contrast, limited biochemical and structural information is available for Hsp110s. Although Hsp110s have the two functional domains such as Hsp70s, it has been enigmatic whether Hsp110s have similar intrinsic activities and allosteric coupling. The ATP binding is essential for the “holdase” activity and NEF activity of Hsp110s (6, 9, 22, 23, 56); however, it has been under debate whether Hsp110s have an active ATPase activity (3, 20, 24, 56–60). For the peptide substrate-binding activity, limited information is available since only a handful of substrates have been identified and analyzed for Hsp110s (41, 61–64). More importantly, how the two functional domains are coupled, *i.e.*, the allosteric coupling, remains largely a mystery. A number of studies suggested that like Hsp70s, Hsp110s have two overall conformations depending on the nucleotides bound: the ATP-bound and ADP-bound/nucleotide-free states (4, 6, 9, 22, 40, 58, 59, 61). Sse1, an Hsp110 from *Saccharomyces cerevisiae*, is the most studied Hsp110 (7, 9, 65). Consistent with the reported functional and physical interaction between the separately expressed domains (6), the crystal structure of Sse1 in complex with ATP has revealed extensive contacts between the two functional domains (40, 56, 66), suggesting an exceptionally strong interaction between the NBD and SBD. In contrast, limited domain contacts have been suggested for the ADP-bound/nucleotide-free state, although no structure is available for this state yet.

A number of studies including two structural analyses on Sse1 in complex with Hsp70s have revealed the molecular mechanism of the NEF activity of Hsp110s and provided support for the importance of the ATP-bound conformation for the NEF activity (22, 56, 66–68). Despite this, however, how allosteric coupling in Hsp110s contributes to the “holdase” and NEF activities is not completely understood. It has been suggested that the ATP-hydrolysis associated allosteric communications in Hsp110s are dispensable for the functional cycle of Sse1 (56, 59, 68). Hsp110s seem to have unique allosteric interactions between the functional domains that are different from those of the classic Hsp70s. Indeed, the relative orientation of the two domains is different to some extent between the crystal structures of Sse1 and Hsp70s in complex with ATP (40, 50, 51). However, the molecular mechanism of this unique allosteric coupling in Hsp110s remains elusive.

To dissect the unique allosteric coupling in Hsp110s, we carried out mutational analysis on Msi3, the only Hsp110 in yeast *Candida albicans* (9, 69, 70). Msi3 shares 63.4% sequence identity with Sse1. Recently, we have purified Msi3 and showed that Msi3 shares almost identical biochemical activities as Sse1 (71). Msi3 has a higher and more consistent expression than Sse1, which made it more suitable for biochemical analysis. We have made three mutations on the

NBD-SBD interfaces and interlobe contacts within the NBD. Biochemical analysis of these mutants suggested that Hsp110s have a unique allosteric regulation underlying their distinctive function in assisting protein folding.

Results

Both the NBD-SBD interfaces and interlobe contacts within the NBD are essential for the function of Msi3, a Hsp110 in *C. albicans*

Previously we solved the first X-ray crystal structure of a full-length Hsp110 using Sse1 (40). This structure revealed extensive and unique interfaces between the two functional domains as well as within the NBD for the ATP-bound state (Fig. 1, A and B). These interfaces could be crucial for the unique allosteric communications and characteristic biochemical properties of Hsp110s. Thus, we mutated these interfaces.

There are mainly two interfaces between NBD and SBD: NBD-SBD β and NBD-SBD α . The NBD-SBD α interface has been suggested to be important for the *in vivo* activity and NEF activity of Sse1 while the role of the NBD-SBD β interface remains elusive (40, 56, 59). To test the NBD-SBD β interface, we mutated L_{2,3}, one of the loops in the SBD β that mediate an important NBD-SBD β contact (Fig. 1B). For testing the NBD-SBD α interface, we took advantage of the previously characterized I163D mutation on this interface (Fig. 1B) (40). Ile163 is highly conserved and the I163D mutation abolishes the *in vivo* function of Sse1.

Additionally, the NBD of Sse1 has a unique structure. Like Hsp70s, the NBD is composed of two large lobes: I and II (Fig. 1B). Between the lobes is a deep cleft where the nucleotide binds. The relative orientation of the two lobes changes between the ATP-bound and ADP-bound structures of Hsp70s (50, 51, 72–74). This orientation change could be a key feature for regulating ATP hydrolysis and allosteric coupling in Hsp70s. For Hsp110s, only the ATP-bound structures are available, and the relative orientation of the two lobes is almost identical to that of the ATP-bound structures of Hsp70s (40, 56, 66, 75). Intriguingly, there are more extensive contacts between the two lobes of NBD for Hsp110s than those of Hsp70s, indicating that the ATP-bound state of Hsp110s is more stable than that of Hsp70s. One unique set of contacts in Sse1 is mediated by Arg235 (Fig. 1, B and C). Arg235, located in lobe II, forms two hydrogen bonds with two residues in lobe I, Asn67 and Glu84. Residues involved in these contacts (Arg235, Asn67, and Glu84) are conserved in Hsp110s (Fig. S1). In Hsp70s, a highly conserved glutamic acid is located at the analogous position of Arg235 (Fig. 1C, bottom panel). More importantly, mutating Arg235 to glutamic acid abolished the *in vivo* function of Sse1 (40). Thus, we used the R235E mutation to test the interlobe contact within the NBD.

Due to the low expression level of the Sse1 proteins carrying either the I163D or R235E mutation, we took advantage of Msi3, the sole and essential Hsp110 in the yeast opportunistic pathogen *C. albicans* (9, 69, 70). Sharing 63.4% sequence identity with Sse1, Msi3 can substitute Sse1 in supporting

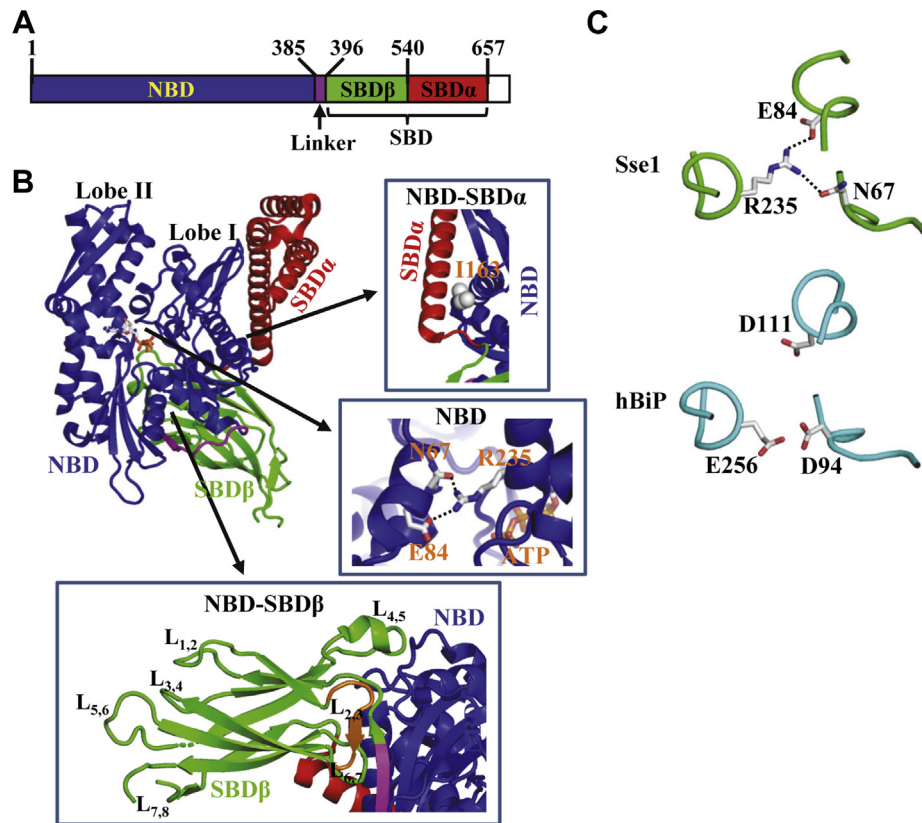


Figure 1. The domain organization and structure of the yeast Hsp110 Sse1. A, the domain organization of Hsp110s. The residue numbers of Sse1 are labeled on the top. B, Ribbon diagram of the Sse1 structure (PDB code: 2QXL). The domain coloring is the same as in A. The bound ATP is highlighted as sticks. On the right are the zoom-in views of the regions involving in I163 on the NBD-SBD α interface (top) and R235 on the interlobe contacts of the NBD (bottom). The hydrogen bonds are shown as dotted lines. The bottom is the zoom-in view of the NBD-SBD β contacts to show the position of L_{2,3} (orange). C, comparison of the Sse1-ATP (top panel) and hBiP-ATP (bottom panel, PDB code: 6ASY) structures on the R235 contacts. The hydrogen bonds are shown as dotted lines.

growth at elevated temperatures (70). Recently, we have purified the wild-type (WT) Msi3 protein and shown that it has almost identical biochemical activities as Sse1 (71). Therefore, we introduced the analogous mutations into Msi3 (Fig. S1). To mutate L_{2,3}, we replaced its sequence (420PKGGLFP426) with a GS linker and named this mutant Δ L_{2,3}. First, we tested whether these mutations affect the *in vivo* function of Msi3. To do this, we used a *S. cerevisiae* strain carrying a deletion of the *SSE1* gene. As shown before (70, 71), the WT *MSI3* gene can rescue the temperature-sensitive phenotype of the *SSE1* deletion strain (Fig. 2A). Consistent with the analogous Sse1 mutations, neither I164D nor R235E was able to support growth at 37 °C, an elevated temperature (Fig. 2A). As predicted by the Sse1 structure, the Δ L_{2,3} mutant abolished the *in vivo* function of Msi3 (Fig. 2A). These mutants were expressed at a similar level as the WT Msi3 (Fig. 2B). Thus, the *in vivo* functional defect is not due to a lack or significant reduction of expression.

To directly confirm the functional defect of these Msi3 mutants, we purified these mutant proteins (Fig. S2) and carried out a refolding assay using an Ssa1 chaperone system containing Ssa1, Msi3, and Ydj1. Hsp110 is an essential component of the Hsp70-Hsp110-Hsp40 chaperone machinery, which is crucial for protein folding, degradation, transportation into organelles, and dismantling protein aggregates (1, 5, 7–9, 18–20, 24–39). Ssa1 is the major Hsp70 in the

cytosol of *S. cerevisiae*. The endogenous Ssa1 chaperone system for protein folding contains Ssa1, Sse1, and Ydj1. Ydj1 is a Hsp40. Recently, we have shown that Msi3 can substitute Sse1 in assisting the refolding activity (71). As shown in Figure 2C, none of the mutant Msi3 proteins were able to significantly increase the refolding of the heat-denatured luciferase above the negative control (without Msi3 protein), supporting the *in vivo* functional defect.

The NBD-SBD allosteric coupling is disrupted in the Msi3 mutants

Based on the locations, we expected that the allosteric coupling in the ATP-bound state is disrupted in all the Msi3 mutants. A number of previous studies, including our limited trypsin digest analysis, have revealed that Hsp110s such as Sse1 have two overall conformational states: the ATP-bound and ADP-bound/nucleotide-free (apo) states (22, 40, 59). Limited proteolysis, short and controlled exposures of proteases such as trypsin, can provide information regarding protein structures and conformational changes. The relatively low concentrations of proteases used in limited proteolysis normally cut at flexible regions exposed on the surface of proteins. The ATP-bound state is more resistant to trypsin digest than the ADP-bound/apo state, consistent with the extensive NBD-SBD contacts

The unique allosteric regulation of Hsp110

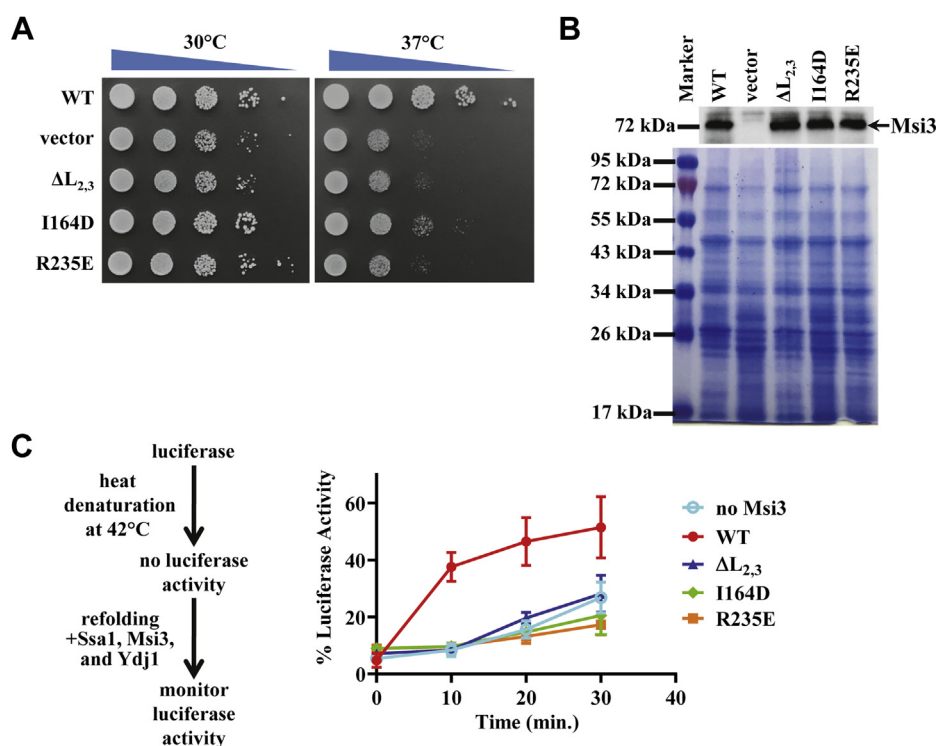


Figure 2. Growth test and the activity of the purified Msi3 proteins in assisting protein refolding. *A*, growth test of the Msi3 mutations were labeled on the left. Serial dilutions of fresh cultures were spotted on agar plates and incubated at 30 and 37 °C. *B*, protein expression levels of the Msi3 mutants at 37 °C. *Top panel*: the Western blot analysis of Msi3 expression levels using an anti-Sse1 antibody. This antibody recognizes Msi3. *Bottom panel*: the Coomassie-stained SDS-PAGE loaded with respective cell lysates to show a similar amount of cell lysate was loaded onto each lane. *C*, the activity of the purified Msi3 proteins in assisting Ssa1-Ydj1 in refolding heat-denatured luciferase. The scheme for the experimental setup is shown on the left. The refolding activity is measured by the recovery of the luciferase activity after heat denaturation. The activity of the undenatured luciferase was set as 100%. The Msi3 mutations were labeled on the right. Refolding without Msi3 was used as a negative control (no Msi3). All the data points were mean \pm SD from three to six independent experiments using more than two different protein purifications although some error bars are too small to be visualized.

with the interdomain linker buried between observed in the crystal structures of the ATP-bound Sse1 (40, 56, 66). The reduced trypsin resistance in the ADP-bound/apo state suggests that there is limited contact between the NBD and SBD in this state. Recently, we have confirmed these two conformational states for Msi3 (71). Thus, we tested how these mutations influence these two conformations of Msi3, especially the ATP-bound state, using the limited trypsin digest analysis. Consistent with the previously published results for Sse1 and Msi3 (40, 71), two signature proteolytic bands were observed in the presence of ATP for the WT Msi3 protein: one at ~43 kD and the other at ~36 kD, most likely corresponding to the NBD and SBD, respectively (Fig. 3). Additionally, there was a significant amount of undigested Msi3 protein. In contrast, in the absence of ATP, there was no visible 43 kD band while the band of ~36 kD was the most prominent digested band. Moreover, there was almost no intact protein left. Instead, several bands slightly smaller than the undigested Msi3 were visible. These bands were also observed for Sse1 and identified as digestions at the N-terminal end.

When we tested the mutant proteins, the signature trypsin digest pattern in the presence of ATP was almost completely abolished (Fig. 3), suggesting that the ATP-bound conformation is specifically compromised in all the mutants. Regardless of the nucleotides, the digest patterns were almost the same for the same mutant protein, suggesting the ATP-induced allosteric

coupling is disrupted. However, there were obvious differences among the mutations. For I164D and R235E, the digest patterns were virtually identical to that of the WT Msi3 in the absence of ATP regardless of whether ATP was present. In contrast, ΔL_{2,3} showed a new digest pattern. The bands slightly smaller than the undigested Msi3 were significantly reduced, as was the band at ~36 kD, suggesting an overall increased sensitivity to trypsin digestion. Taken together, the loss of the ATP-bound state for all the mutants is consistent with our structural prediction.

The Msi3 mutants exhibit a reduced affinity for ATP but an increased affinity for peptide substrate

Based on the Sse1-ATP structure, all the mutations are quite far away from the ATP-binding site in the NBD, especially ΔL_{2,3}, which is in the SBD (Fig. 1B). We expected that none of these mutations would have significant influence on ATP binding if the NBD-SBD allosteric coupling had little influence on the binding of ATP. To test ATP binding, we carried out a fluorescence polarization assay using ATP-FAM, a fluorescent-labeled ATP. Using this assay, we have recently shown that Msi3 binds ATP-FAM with high affinity (71). As shown in Figure 4, A and B, the affinity of Msi3 for ATP-FAM is about 40-fold higher than that of Ssa1. Surprisingly, all the mutations showed significantly reduced affinities for ATP-FAM (Fig. 4, A and B). The reduced affinity of ATP-FAM for I164D and ΔL_{2,3}

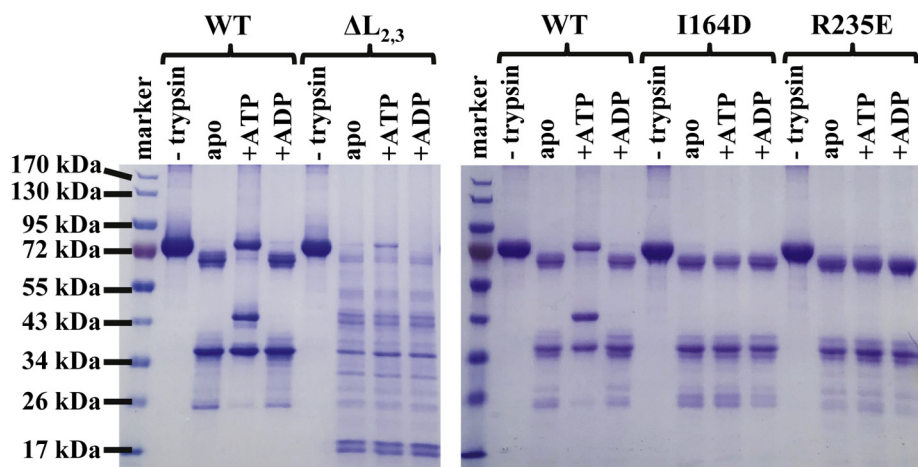


Figure 3. The Msi3 mutant proteins showed defects in the ATP-dependent allosteric coupling. The ATP dependence of proteolytic susceptibility was compromised in the Msi3 mutant proteins. Msi3 proteins were treated with a low concentration of trypsin in the presence and absence of ATP or ADP. The Coomassie-stained SDS-PAGE was used to visualize the digestion profiles. WT: the wild-type Msi3. apo: no nucleotide added; +ATP: ATP was added; +ADP: ADP was added.

suggested that the NBD-SBD contacts influence the ATP-binding affinity of the NBD, further supporting the allosteric defect observed above in the trypsin digest assay. Although compromised, significant ATP binding was observed for all the Msi3 mutant proteins. Under the physiological concentration of ATP (1–10 mM) and the ATP concentration used in the trypsin digest (1 mM), the ATP binding is supposed to be saturated for all the Msi3 mutants. Thus, the defective ATP-binding state observed above in all the Msi3 mutant proteins most likely is not caused by a lack of ATP binding.

Next, we tested the substrate-binding affinities of these Msi3 mutants. Previously, we have shown that the TRP2 peptide binds to Hsp110s, whereas Hsp110s showed little binding to the NR peptide, a well-established peptide substrate for Hsp70s (58). The amino acid sequences of these two peptides were shown in Table 1. The TRP2_181 peptide is a longer version of the TRP2 peptide and showed a stronger binding to Hsp110s than the TRP2 peptide. Consistent with these observations, Msi3 bound the TRP2_181 peptide with a high affinity, whereas little binding to the NR peptide was detected (Fig. 4, C and D, and S3A). In addition, ATP binding reduced the binding affinity for the TRP2_181 peptide, whereas ADP has little influence (Fig. 4, C and D), consistent with the reported ATP sensitivity of the peptide substrate binding for Hsp110s and the ATP-induced allosteric coupling in Msi3. When we tested the mutant proteins, all showed increased affinities for the TRP2_181 peptide to different levels (Fig. 4D and S3, B–D). Moreover, the ATP sensitivity was largely lost, which is consistent with the loss of the ATP-bound state and allosteric coupling in these mutants revealed by the above limited trypsin digest analysis.

Msi3 has a cryptic ATPase activity that is suppressed mainly by the NBD-SBD β contacts

A number of studies including our biochemical and crystallographic analysis suggest that the full-length Sse1 has little

ATPase activity (40, 56–59), while other studies have demonstrated a significant ATPase activity for Hsp110s (3, 20, 24, 60). Using the isolated NBD of Sse1 and chimera constructs between Sse1 and a Hsp70, a recent study suggested that Sse1 has a cryptic ATPase activity that is not shown by the full-length Sse1 alone and is suppressed by the NBD-SBD contacts (59). To directly test whether a full-length Hsp110 has an ATPase activity and how the NBD-SBD contacts or the interlobe contacts within the NBD influence the ATPase activity, we analyzed the ATPase activities of the Msi3 mutants. One factor causing discrepancy in the literature on whether Hsp110 has an active ATPase activity is the assays used. All the studies that showed ATPase activity for Hsp110s utilized the steady-state ATPase assay; whereas the single-turnover ATPase assay was used for the studies that support little ATPase activity. The single-turnover ATPase assay is much less influenced by contaminating proteins than the steady-state ATPase assay. In general, the single-turnover ATPase assay produces more accurate and consistent results than the steady-state ATPase assay. Moreover, the single-turnover ATPase assay is able to accurately determine a wide range of ATPase activities (76, 77). Thus, we carried out a single-turnover ATPase assay.

As shown in Figure 4E, the full-length Msi3 had little ATPase activity. This is consistent with our published results on Sse1 (40, 58). Interestingly, $\Delta L_{2,3}$ showed a significant ATP hydrolysis, whereas very limited ATP hydrolysis was observed for I164D and R235E. The ATPase rate of the $\Delta L_{2,3}$ mutants ($5.64 \pm 1.12 \times 10^{-3}/\text{min}$) is about 7-fold lower than that of Ssa1 reported at the same temperature (58). Thus, these data support a cryptic ATPase activity for the full-length Msi3. However, this ATPase activity is autoinhibited, mainly by the NBD-SBD β contacts. This is because only $\Delta L_{2,3}$ with compromised NBD-SBD β contacts showed an ATPase activity, whereas disrupting either the NBD-SBD α contacts by the I164D mutation or the interlobe contacts within the NBD by the R235E mutation has little influence on the ATPase

The unique allosteric regulation of Hsp110

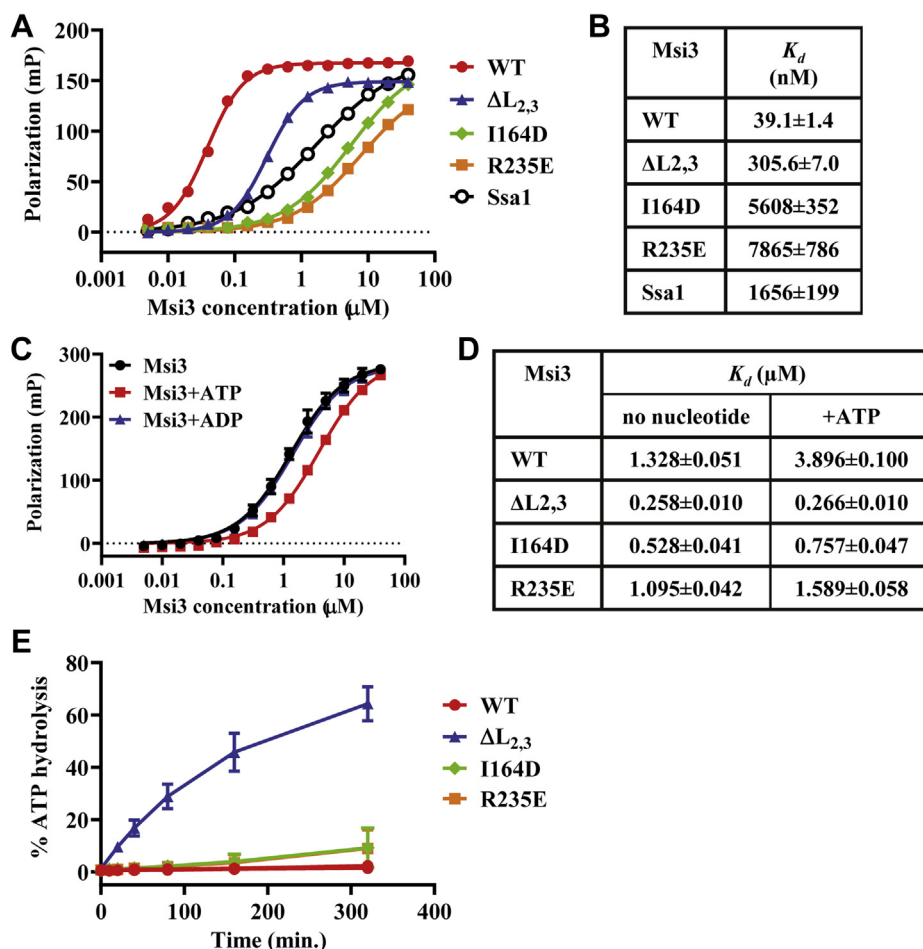


Figure 4. The intrinsic activities of the Msi3 mutant proteins. A, the Msi3 mutant proteins exhibited reduced affinities for ATP. The ATP binding to the Msi3 proteins was assayed using fluorescence polarization with ATP-FAM. B, The dissociation constants (K_d) deduced from A. C, the WT Msi3 protein binds the TRP2 peptide in an ATP-dependent manner. The TRP2 peptide was labeled with fluorescein at the N-terminus. Fluorescence polarization assay was carried out after the binding reached equilibrium. Msi3: no nucleotide was added; Msi3+ATP: ATP was added; Msi3+ADP: ADP was added. D, the dissociation constants (K_d) of the Msi3 mutants for the TRP2_181 peptide. The WT data were deduced from C. The corresponding binding data for the mutants were shown in Figure S3. E, the ATPase activity was influenced differently by the mutations in Msi3. The ATPase activity of Msi3 proteins was measured using the single-turnover ATPase assay. The deduced catalytic constant (k_{cat}) for the ΔL_{2,3} mutant is $5.64 \pm 1.12 \times 10^{-3}$ /min. The ATP hydrolysis for the rest of the Msi3 proteins was too low to calculate k_{cat} . The percentages of ATP hydrolysis were plotted as a function of reaction time (mean ± SD from three to five independent experiments using more than two different protein purifications).

activity. This cryptic ATPase is consistent with the reported ATPase activity of the isolated NBD of Sse1 although at much lower rate (59).

The “holdase” activity was largely intact for all the Msi3 mutants

Hsp110s have been shown to have a strong activity in preventing protein aggregation, the “holdase activity” (18–21). Using the heat-denatured firefly luciferase as the substrate, we

recently showed that Msi3 also has this activity (71). Next, we tested whether the holdase activity of Msi3 was affected in the Msi3 mutants. Consistent with the published results, upon incubation at 42 °C, an elevated temperature, the firefly luciferase showed an increasing OD reading at 320 nm, an indication for protein aggregation (Fig. 5A). In the presence of ATP, addition of Msi3 was able to significantly reduce this heat-induced aggregation of luciferase, *i.e.*, Msi3 can prevent the luciferase from aggregating. Msi3 showed limited aggregation by itself upon incubation at 42 °C (Fig. 5B). As shown before for both Sse1 and Msi3 (19, 71), this “holdase” activity is ATP-dependent since in the absence of ATP or the presence of ADP, this activity was lost (Figs. 5C and S4A), suggesting that the ATP-bound conformation is required for this activity.

When we tested the mutations, surprisingly, all the three mutant proteins were able to suppress the aggregation of luciferase to a similar level as that of the WT Msi3 in the presence of ATP. Moreover, like the WT Msi3, none of these

Table 1
The peptide substrates used for Hsp110s and Hsp70s

Name	Sequence
NR	NRLLLTG
TRP2	SVYDFFVWL
TRP2_181	VYDFFVWLHYY
TRP2-Bpa	SVYDFFVBpaLK

All the peptides were labeled with fluorescein at the N-terminus. No further modification was made to any of the peptides.

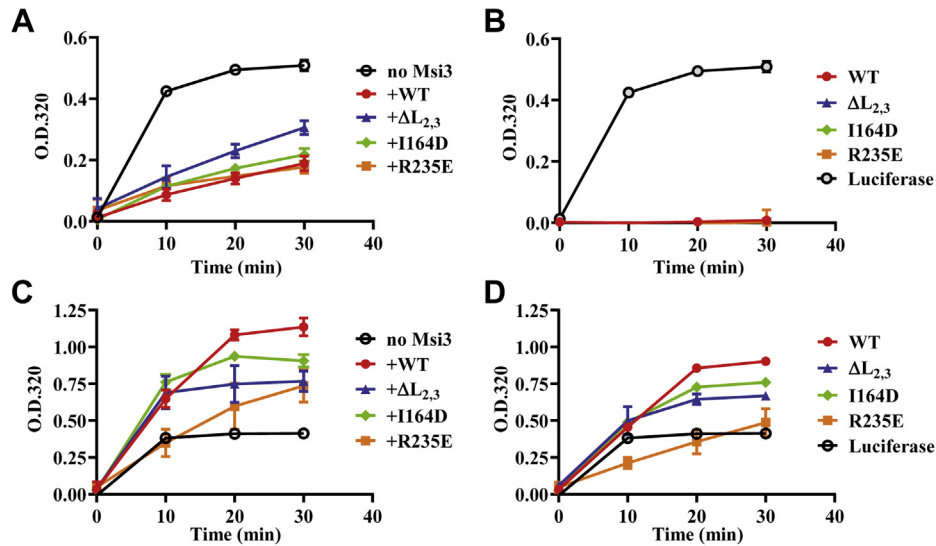


Figure 5. The preventing aggregation activity of the Msi3 mutant proteins. A and C, the preventing aggregation activity of Msi3 proteins in the presence of (A) and absence of ATP (C). Firefly luciferase was used as a model substrate. Heating at 42 °C results in luciferase aggregation as measured by increased readings at O.D. 320 nm. Luciferase alone was used as a negative control (no Msi3). The additions of Msi3 WT and mutant proteins were labeled on the right of each plot. B and D, the aggregation of the Msi3 proteins alone in the presence of (B) and absence of ATP (D). The aggregation of luciferase alone was used as a control (Luciferase). All data were mean \pm SD from three independent experiments using more than two different protein purifications.

mutant proteins showed significant aggregation by itself upon heating at 42 °C in the presence of ATP. In the absence of ATP or presence of ADP, like the WT Msi3, none of the mutant proteins were able to suppress the aggregation of luciferase (Figs. 5C and S4A). In addition, all the Msi3 proteins showed increased aggregation in the absence of ATP or presence of ADP (Figs. 5D and S4B). The clear differences in OD readings between in the presence and absence of ATP for all the mutants suggested that there is still some allosteric coupling although strong defects in allosteric coupling were detected by the limited trypsin digest analysis. Furthermore, the presence of ADP showed almost identical results as those in the absence of ATP (Fig. 5, C and D and S4, A and B), consistent with the virtually indistinguishable tryptic patterns for these two states.

Taken together, for the “holdase” activity, although the ATP-induced allosteric coupling is required, it can tolerate significant disruptions on all the interfaces tested in this study. This could be due to the exceptionally strong NBD-SBD contacts in Hsp110s. Since $\Delta L_{2,3}$ showed a “holdase” activity close to the WT level, autoinhibiting the hidden ATPase activity seems not required for the “holdase” activity of Msi3. Furthermore, although ATP binding is required, it appeared that the reduced ATP-binding affinity in all the mutants had no appreciable effect on the “holdase” activity. Taken together, the “holdase” activity seems a very robust and forbearing activity.

All the Msi3 mutations compromised the NEF activity

Hsp110s have been shown to function as the major nucleotide-exchange factor (NEF) for Hsp70s (3, 4, 9, 22, 23). The ATP-bound state of Hsp110s is important for this NEF activity although a mutational analysis suggested that the NBD-SBD β contacts seem to be dispensable for the

NEF activity (6, 9, 22, 23, 56). We tested whether the NEF activity of Msi3 was affected by the mutations in order to dissect how each interface influences the NEF activity.

Consistent with our recent study on Msi3 (71), Msi3 is able to function as an NEF for Ssa1 (Fig. 6A). In this assay, we first formed a complex of Ssa1 with ATP-FAM. This complex had a high polarization reading due to the large size of Ssa1. Adding either buffer or Msi3 alone only resulted in very slow decreasing of polarization values (Fig. 6B). Upon adding the unlabeled ATP, the polarization reading decreased over time, indicating the bound ATP-FAM was slowly replaced by the unlabeled ATP, *i.e.*, the nucleotide exchange (Fig. 6, A and B). In contrast, adding Msi3 in combination with the unlabeled ATP caused a drastically accelerated release of the bound ATP-FAM as indicated by the fast decrease of polarization readings, *i.e.*, the NEF activity (Fig. 6A).

When we tested the mutants, all showed a compromised NEF activity (Fig. 6). Compared with the “holdase” activity tested above, the NEF activity of Msi3 is more sensitive to the ATP-induced allosteric coupling. Thus, the NEF activity depends on the ATP-bound state and allosteric coupling of Msi3. This is consistent with the published studies on Sse1 (22, 56, 68). However, there was significant difference among the mutations. The NEF activity was almost completely abolished for I164D and R235E (Fig. 6, A–C). In contrast, $\Delta L_{2,3}$ showed some significant NEF activity although lower than that of the WT. This result suggested that the NEF activity is more dependent on the NBD-SBD α interfaces and interlobe contacts within NBD than the NBD-SBD β interfaces. This is consistent with the crystal structures of Sse1 in complex with Hsp70s, which have shown that Sse1 interacts with Hsp70s mainly through Sse1’s NBD and SBD α (56, 66).

The unique allosteric regulation of Hsp110

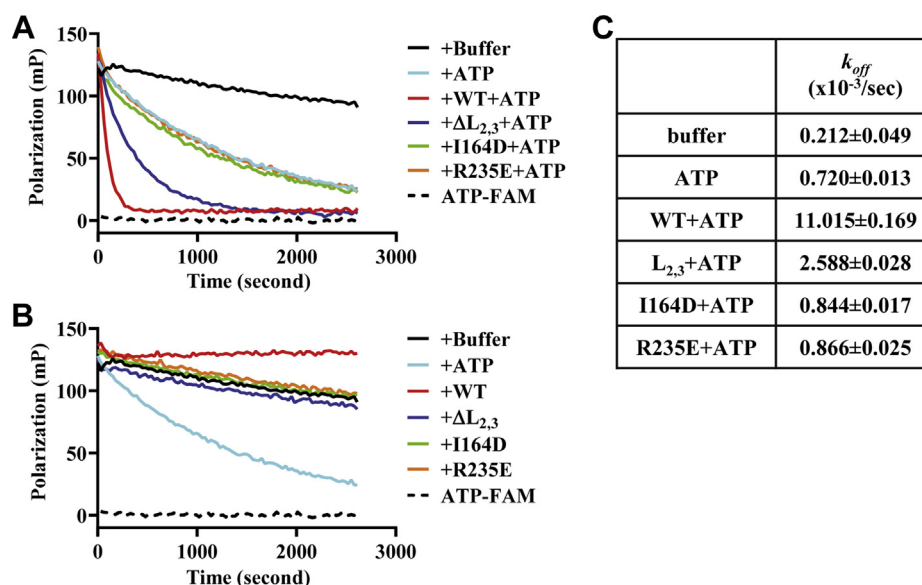


Figure 6. The NEF activity of the Msi3 mutant proteins. A and B, the release of the bound ATP-FAM from the Ssa1 protein in the presence (A) and absence (B) of ATP. Addition of ATP (+ATP) or buffer (+buffer) alone was used as control. The polarization reading of ATP-FAM alone was set as zero. C, the calculated dissociation constants (k_{off}) from A and B.

Stable peptide substrate binding to Msi3 disrupted the interdomain contacts and compromised the Msi3-Ssa1 interaction but had little impact on the cryptic ATPase activity

For Hsp70s, it is well established that the binding of peptide substrate dissociates the NBD-SBD contacts and thus stimulates the intrinsic ATPase activity (10, 13, 43, 49, 78). Then, we tested whether peptide substrates influence the allosteric coupling and cryptic ATPase activity of Msi3. Unlike Hsp70s, limited information is available for Hsp110s in terms of peptide substrates. Up to now, only two peptide substrates have been reported to bind Sse1, the TRP2 and LIC peptides (58, 61). We have shown that the TRP2 peptide binds Msi3 in a similar fashion as Sse1 in this study (Fig. 4, C and D). However, when we analyzed the allosteric coupling in Msi3 using the limited trypsin digest, no appreciable difference was observed when the TRP2 peptide was added (Fig. 7A). Consistent with this result, no ATPase stimulation was observed by either the TRP2 or LIC peptide (58, 61).

Since the peptide binding is transient for Hsp110s (58), we reasoned that a stable complex with a peptide substrate could be the key to induce conformational changes in Hsp110s. To stabilize an Msi3-peptide complex, we took advantage of the TRP2-Bpa peptide, a derivative of the TRP2 peptide (sequences shown in Table 1) (79). The TRP2-Bpa peptide contains a p-benzoyl-L-phenylalanine (Bpa), an unnatural amino acid, replacing the tryptophan in the original TRP2 peptide. Since Bpa and tryptophan share a similar structure, we expected that the TRP2-Bpa peptide shares a similar property as the TRP2 peptide in binding to Hsp110s. As expected, both Msi3 and Sse1 showed significant binding to the TRP2-Bpa peptide and ATP binding reduced the affinity (Fig. S5), consistent with the ATP sensitivity of the substrate binding. Importantly, upon UV treatment, a significant amount of the TRP2-Bpa peptide was cross-linked to the Msi3 protein in a

concentration dependent manner (Fig. 7B). Since the isolated NBD of Sse1 is not stable and difficult to express for purification (6), we used the isolated NBD of DnaK as a negative control. When treated with the TRP2-Bpa peptide, little cross-linking was observed for the NBD of DnaK as reported previously (79). The strong cross-linking bands suggested that a covalent and specific complex was formed between Msi3 and the TRP2-Bpa peptide.

Importantly, the ATP-dependent resistance to trypsin digest was compromised when Msi3 was cross-linked with the TRP2-Bpa peptide (Fig. 7C), whereas neither UV treatment alone nor the treatment with the solvent DMF, which the TRP2-Bpa peptide was dissolved in, had observable influence on the ATP-dependent resistance to trypsin digest. Additionally, the NR peptide also exhibited little effect on the trypsin digest pattern, consistent with the lack of binding to Hsp110s including Msi3 (Fig. S3A for Msi3) (58). Thus, the loss of the ATP-dependent resistance to the trypsin digest is specific when Msi3 is cross-linked to the TRP2-Bpa peptide.

When we tested the ATPase activity using the single-turnover ATPase assay after cross-linking with the TRP2-Bpa peptide, very limited ATP hydrolysis was observed (Fig. 8A). UV treatment alone had no apparent impact on the ATPase activity. Thus, although cross-linking the TRP2-Bpa peptide resulted in loss of the ATP-bound state and defect in NBD-SBD coupling for Msi3, the cryptic ATPase remained suppressed.

Next, we tested how peptide substrate binding to Msi3 influenced the NEF activity, *i.e.*, the functional interaction with Ssa1. Since both the TRP2-Bpa peptide and ATP-FAM are labeled with fluorescein-derived fluorophores, we were not able to analyze the NEF activity directly. It was shown that Sse1 and Ssa1 form a stable complex and the complex formation is consistent with the NEF activity (5, 24, 56, 80). Thus,

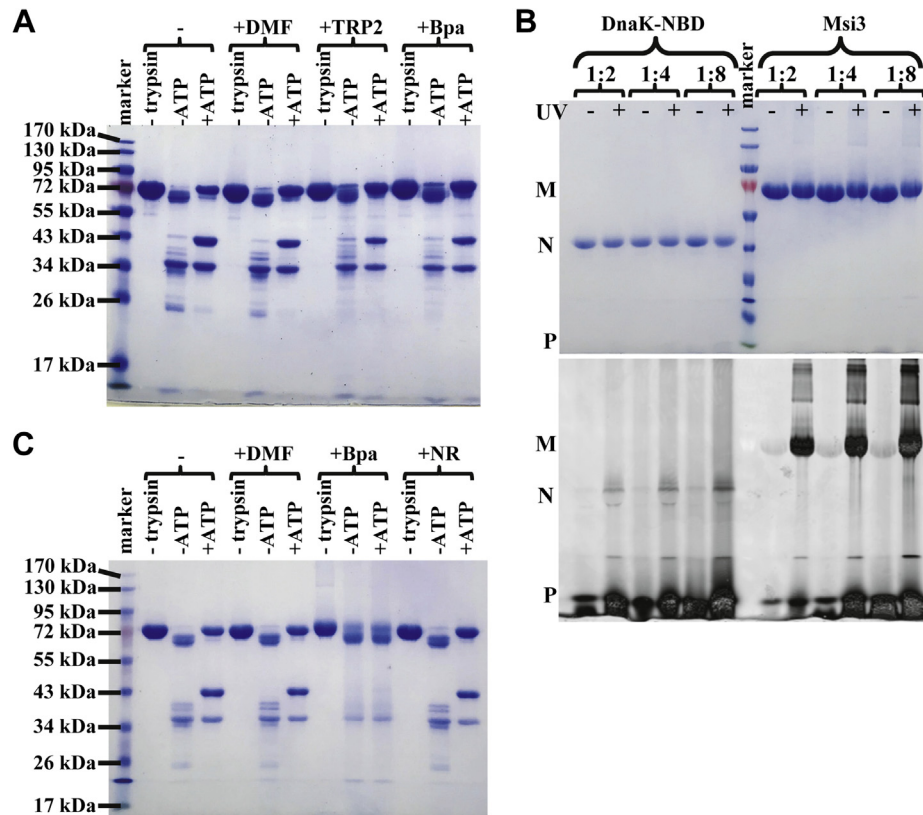


Figure 7. Stable peptide substrate binding dissociates the NBD-SBD contacts in Msi3. A, peptide substrates have little influence on the proteolytic susceptibility of Msi3. The Msi3 protein was treated with trypsin in the presence of either the TRP2_181 (+TRP2) or TRP2-Bpa (+Bpa) peptide. DMF was used as a control (+DMF). B, the TRP2-Bpa peptide was specifically cross-linked to the Msi3 protein. The Msi3 protein (1 mg/ml) was incubated with the TRP2-Bpa peptide at the indicated molar ratios and treated with UV light (365 nm) for cross-linking. The isolated NBD of DnaK was used as a negative control. After separating on a SDS-PAGE, the cross-linked Msi3-peptide complex was visualized by Coomassie Blue stain (top) and fluorescence scan (bottom), respectively. N: the isolated NBD of DnaK; M: Msi3; P: the TRP2-Bpa peptide. The sizes of proteins in the marker are: 170, 130, 95, 72 (red), 55, 43, 34, 26, and 17 kDa, respectively, from top to bottom. C, the cross-linked TRP2-Bpa peptide abolished the ATP-dependence of the proteolytic susceptibility of Msi3. After cross-linking with the TRP2-Bpa peptide (+Bpa), the Msi3 protein was treated with trypsin in the presence and absence of ATP. All the Msi3 proteins were treated with UV light (365 nm). Samples incubated with DMF (+DMF) and the NR peptide (+NR) were used as controls.

we analyzed the Msi3-Ssa1 complex formation using a native gel. A number of previous studies have shown that the ATP-binding and ATP-bound state of Sse1 is essential for forming the Hsp70-Hsp110 complex (22, 56, 80). Consistent with these observations, a strong complex band was formed between Msi3 and Ssa1 in the presence of ATP. As shown in Figures 7C and 8A, cross-linking the TRP2-Bpa peptide to Msi3 resulted in loss of the ATP-bound conformation although the cryptic ATPase activity was still suppressed. Thus, we hypothesized that cross-linking the TRP2-Bpa peptide to Msi3 would disrupt the complex formation between Msi3 and Ssa1. Interestingly, in support of our hypothesis, the Msi3-Ssa1 complex band was drastically reduced after Msi3 was cross-linked to the TRP2-Bpa peptide (Figs. 8B and S6) while UV treatment alone had little impact on the formation of the complex. Without UV cross-linking, the complex formation was largely unaffected, consistent with the lack of influence on the tryptic digest pattern. An interesting observation is that the TRP2-Bpa peptide did not comigrate with the Msi3-Ssa1 complex band even though the TRP2-Bpa peptide was efficiently cross-linked to the Msi3 protein (Fig. S6), suggesting that once a stable complex between the Msi3 protein and the TRP2-Bpa peptide was formed through cross-linking, this

Msi3-peptide complex would not be able to bind Ssa1. The residual band for the Msi3-Ssa1 complex most likely was formed by Msi3 without cross-linking to the TRP2-Bpa peptide.

The influence of the TRP2-Bpa peptide on the Msi3-Ssa1 complex is in stark contrast with the NR peptide. When Msi3 was incubated with the NR peptide, the amount of the NR peptide that comigrated with Msi3 was almost nondetectable (Figs. 8B, S6 and S7), consistent with little binding between Msi3 and the NR peptide (Fig. S3A). In contrast, a significant amount of NR peptide comigrated with Ssa1 (Figs. 8B, S6 and S7). This is consistent with the published results that the NR peptide binds to Hsp70s including Ssa1 with high affinities (58). Consistent with the previous studies, Ssa1 formed multiple bands on the native gel, suggesting the formation of oligomers besides the monomer form (the position was labeled on the native gel). Incubating with the NR peptide shifted Ssa1 to mainly the monomer form, which the NR peptide comigrated with as supported by the fluorescence scan, suggesting that the monomer form of Ssa1 formed a stable complex with the NR peptide. Importantly, regardless of whether the NR peptide was first incubated with Msi3 or Ssa1, a strong Msi3-Ssa1 complex band was observed, and the amount was

The unique allosteric regulation of Hsp110

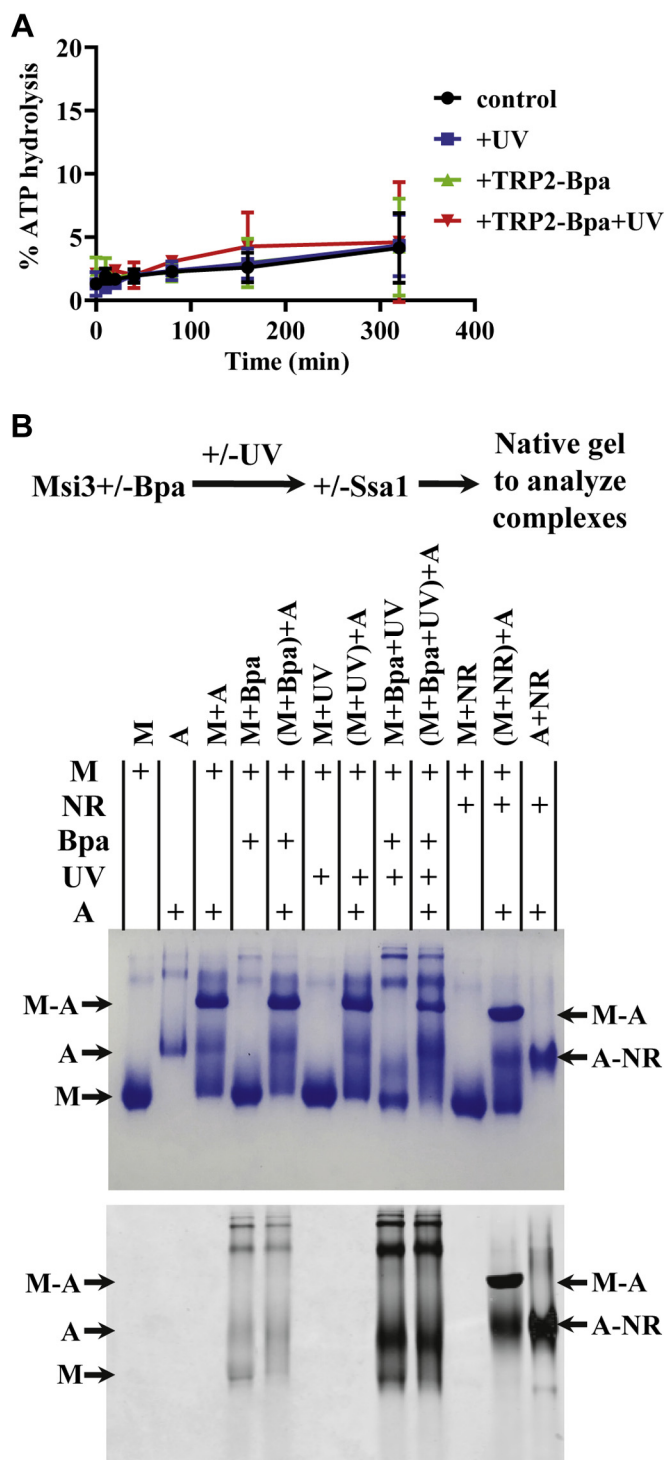


Figure 8. The effects of peptide substrate on the ATPase activity of Msi3 and the formation of the Msi3-Ssa1 complex. A, peptide substrate showed little influence on the ATPase activity of Msi3. The single-turnover ATPase assay was carried out on the Msi3 protein with and without cross-linked to the TRP2-Bpa peptide (+TRP2-Bpa+UV and +TRP2-Bpa, respectively). No UV treatment (control) and UV treatment alone (+UV) were used as controls. The percentages of ATP hydrolysis were plotted as a function of reaction time (mean \pm SD from three independent experiments using more than two different protein purifications). B, cross-linking of the TRP2-Bpa peptide to Msi3 reduced the formation of the Msi3-Ssa1 complex. Native gel was used to analyze the formation of the Msi3-Ssa1 complex in the presence of peptide substrates. The experimental scheme is shown on the top of the gels. For the samples with the NR peptide, the NR peptide was used in place of the TRP2-Bpa peptide and UV treatment was not applied.

comparable to that in the absence of the NR peptide (Fig. S7). Furthermore, the NR peptide comigrated with the Msi3-Ssa1 complex band as shown by the fluorescence of the NR peptide (Figs. 8B and S7A), suggesting the formation of an Msi3-Ssa1-NR triple complex. Since Msi3 showed little binding to the NR peptide, the NR peptide most likely binds to Ssa1 in this triple complex.

Discussion

In this study, we have made three Msi3 mutations on the NBD-SBD interfaces and the interlobe contacts within the NBD. Using these mutations, we have characterized the role of each interface in the unique ATP-induced allosteric coupling of Hsp110s (Fig. 9). Consistent with the Sse1 crystal structure, all these Msi3 mutations compromised the ATP-bound state and NBD-SBD allosteric coupling. The almost null defect in both *in vivo* and *in vitro* function of the Msi3 mutants supports the importance of these interfaces and the ATP-induced allosteric coupling of Hsp110s. In what seems to be a paradox, all the mutant Msi3 proteins showed an almost WT-level activity in preventing protein aggregation, *i.e.*, the “holdase” activity. However, the “holdase” activity is strictly ATP-dependent for both the WT and mutant proteins. Thus, there must be some residual NBD-SBD contacts in these mutants that are sufficient to support the “holdase” activity. Moreover, all the mutants have a significantly reduced affinity for ATP, suggesting that the NBD-SBD contacts enhance the ATP-binding affinity, another allosteric coupling feature that is different from the classic Hsp70s. Therefore, Hsp110s including Msi3 must have unique and exceptionally strong NBD-SBD contacts that determine the distinctive allosteric coupling and biochemical properties to suit for their specific function.

Previous biochemical and structural analyses have provided support for these remarkably strong NBD-SBD contacts in Hsp110s, especially the reported domain interaction in *trans* (6, 22, 40, 56, 66). Even for the NEF activity, the $\Delta L_{2,3}$ mutant still showed significant activity. $\Delta L_{2,3}$ and I164D directly compromised the NBD-SBD allosteric coupling through disrupting the NBD-SBD β and NBD-SBD α interfaces, respectively, whereas the allosteric defect in the R235E mutant is most likely due to the destabilization of the NBD conformation in the ATP-bound state. Both I164D and R235E abolished the NEF activity, suggesting that the NBD-SBD α contacts and the NBD conformation are more important for interacting with Hsp70 than the NBD-SBD β contacts. This is consistent with the crystal structures of Sse1 in complex with Hsp70s, in which both the NBD and SBD α of Sse1 form contacts with

Top panel: Coomassie Blue stain to visualize proteins; *bottom panel:* fluorescence scan to detect the fluorescence-labeled peptides and chaperone-peptide complexes. The samples were labeled on the top of the gels. The parenthesis indicated that the components inside the parenthesis were incubated first, and then the component outside of the parenthesis was added and incubated. M: Msi3; A: Ssa1; M-A: the complex of Msi3 and Ssa1; NR: the NR peptide; Bpa: the TRP2-Bpa peptide; A-NR: the complex of Ssa1 and the NR peptide.

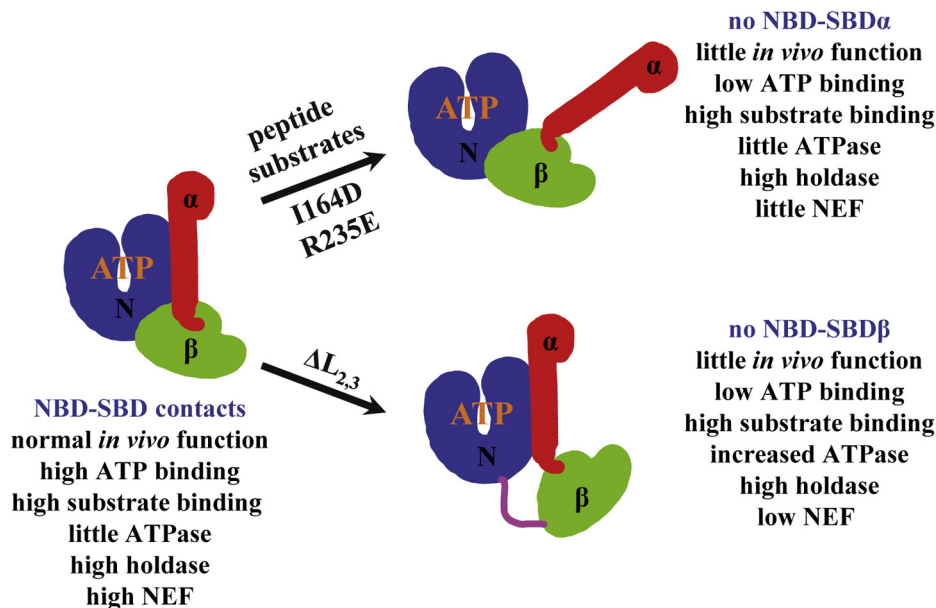


Figure 9. A summary of the unique interdomain coupling in Msi3. The colors and labels for the domains of Msi3 are: NBD (blue, N); SBD β (green, β); SBD α (red, α); and interdomain linker (magenta). For the WT Msi3, there are extensive NBD-SBD contacts (the model on the left). The NBD-SBD β contact is disrupted by the $\Delta L_{2,3}$ mutation (the model on the bottom right). The I164D and R235E mutations as well as stable peptide substrate binding dissociate the NBD-SBD α contacts (the model on the top right). The function and biochemical activities are summarized next to each model.

Hsp70, whereas there is little contact between Sse1's SBD β and Hsp70 (56, 66). All the mutations abolished both the *in vivo* function in supporting growth at elevated temperatures and the *in vitro* activity of Msi3 in assisting the folding activity of Hsp70. Despite a significant NEF activity and almost WT-level "holdase" activity, $\Delta L_{2,3}$ failed to show significant function both *in vivo* and *in vitro*. This is consistent with the previous studies showing that the NEF activity of Msi3 is crucial. A previous study reported two Sse1 mutations on the NBD-SBD β interface. However, different from the $\Delta L_{2,3}$ mutant, neither mutants affected either the *in vivo* function or the NEF activity of Sse1 (56). From this, it was proposed that the allosteric rearrangements induced by ATP hydrolysis seem dispensable for the functional cycle of Sse1. It is possible that these two mutations are not strong enough to influence the NBD-SBD β contacts due to the exceptionally strong interfaces.

It is increasingly recognized that chaperones, such as Hsp70s, and cochaperones are modified by posttranslational modifications (PTMs), the "chaperone code" (81). The PTMs further adjust the chaperone activities of Hsp70s in response to various cellular conditions. It is possible that the unique NBD-SBD contacts of Hsp110s are also modulated by PTMs such as phosphorylation. In fact, there are two serine residues in the $L_{2,3}$ of Sse1 and both have been shown phosphorylated (https://gpmdb.thegpm.org/_/ptm_png/1=YPL106C) although these serine residues are not conserved in Msi3 (Fig. S1).

In contrast, the functional importance of the "holdase" activity remains a mystery. Hsp110s are much larger in size than all other known classes of NEFs. Importantly, they have demonstrated high "holdase" activity by themselves through direct binding to polypeptide substrates, even higher than classic Hsp70s (18–20, 30, 34, 58, 62). It is not surprising that knockdown of Hsp110s but not unrelated NEF has been

shown to result in increased protein aggregation and drastically reduced life span under stress conditions (31), hinting an important function of the "holdase" activity. A mutation that specifically compromises the "holdase" activity is crucial for dissecting the enigma behind this function. Such mutation may be difficult to isolate due to the strong interdomain contacts and robust nature of the "holdase" activity.

An observation of note is the reduced ATP-binding affinity in all the Msi3 mutants, especially I164D and $\Delta L_{2,3}$. I164 and $L_{2,3}$ are both far away from the nucleotide-binding site (Fig. 1B). The reduced ATP-binding affinity must be indirect, most likely through affecting allosteric coupling. Thus, the NBD-SBD contacts most likely enhance the ATP-binding affinity to the NBD. This observation is consistent with the published result that the isolated NBD of Sse1 is not stable (6). It is possible that the NBD-SBD contacts are required to enable the high-affinity binding of ATP for Hsp110s, thus stabilizing the NBD. A similar effect on ATP binding has not been reported for Hsp70s. This property may contribute to the unique allosteric coupling of Hsp110s.

This study provided direct support for a cryptic ATPase activity for Msi3 in the context of a full-length protein. This cryptic ATPase appears to be mainly suppressed by the NBD-SBD β contacts, whereas compromising either the NBD-SBD α interface by I164D or the interlobe contacts within the NBD by R235E showed little release of this cryptic ATPase activity. After disrupting the NBD-SBD β contacts by the $\Delta L_{2,3}$ mutation, the ATPase rate is about 7-fold lower than that of Ssa1. This ATPase rate may be indicative of an only partly released ATPase activity of Hsp110s. This could provide a possible explanation for the discrepancy in the reported ATPase rates of Hsp110s. Throughout the literature, there is no consensus on the rate of the ATPase activity of Hsp110s. This is different

The unique allosteric regulation of Hsp110

from Hsp70s' ATPase activity, which shares a similar rate. Kumar *et al.* reported that the ATPase activity of Sse1 is negligible, whereas the ATPase rate of the isolated NBD of Sse1 is about 16-fold higher than Ssa1 (59). We previously reported the ATPase activity of Sse1 is almost nondetectable (58). In contrast, Mattoo reported that the ATPase activity of Hsp110 is quite similar to that of Hsp70 (20), whereas a study from the Mayer group showed the ATPase activity of WT Sse1 is about 4-fold higher than that of the human Hsc70 (60). It seems that the quality and state of the purified Hsp110 proteins are the key since compromising the NBD-SBD β interfaces may release this ATPase activity at least partially.

The key questions are: when is this cryptic ATPase activity activated under physiological conditions and what is the functional importance of this ATPase activity? A previous study from the Morano group showed that a number of mutations predicted to abolish ATP hydrolysis had little influence on the *in vivo* activity of Sse1, suggesting the ATPase activity is dispensable for the chaperone activity of Hsp110s (6). These mutations were predicted based on the structural and biochemical analysis of Hsp70s. However, most of these mutations are subtle changes such as D8N, D203N, and K69Q. It is possible that changes of these mutations are too minute to cause significant impacts on the ATPase activity of Sse1 but are significant enough to reduce the ATPase activity of Hsp70s. A K69M mutation, a more drastic alternation, has been shown to have a reduced activity in accelerating Hsp104-independent protein disaggregation (28) although little influence was observed in either the *in vivo* function of Sse1 (3, 60) or a number of essential chaperone activities (31, 82, 83), suggesting some importance of the ATPase activity. A mutation that only compromises the ATPase activity is required to clarify the importance of this ATPase activity.

Analogous to the mysterious holdase activity, the functional importance of Hsp110's peptide substrate binding has been elusive. The substrate-binding properties and binding site for Hsp70s are well-characterized (49, 78, 84–87). Comparatively, limited information is available for the substrate properties of Hsp110s since only a handful of substrates have been analyzed for Hsp110s (58, 61, 62, 64). With a recent study suggesting that the substrate binding is not obligate for the biological activity of Sse1 (88), even the importance of substrate binding is under debate. Interestingly, a recent study suggested that the metazoan Hsp110s but not the yeast Hsp110s have a second novel binding site for substrates in the C-terminal extension, adding another layer of complexity to the substrate-binding properties of Hsp110s (41).

Two peptide substrates have been found for Sse1 (58, 61); however, neither stimulate the ATPase activity although the denatured luciferase has been shown to increase the ATPase activity of Hsp110 (20). Since Hsp110s bind peptide substrate transiently, we have cross-linked the TRP2-Bpa peptide to Msi3 to form a stable complex. Although the ATP-bound state is disrupted by this cross-linking as shown by the limited trypsin digest result, the ATPase activity remained almost fully suppressed. Intriguingly, the trypsin digest pattern of the TRP2-Bpa cross-linked Msi3 looked quite similar to those of

the I164D and R235E, consistent with the suppression of the cryptic ATPase activity in these mutations. Thus, cross-linking the TRP2-peptide most likely only dissociates the NBD-SBD α interfaces while the NBD-SBD β interfaces remain largely intact. This is different from Hsp70s, for which peptide substrate binding dissociates both NBD-SBD β and NBD-SBD α contacts (43). The R235E mutation most likely influences the NBD conformation and thus affects the allosteric coupling. Since the limited trypsin digest pattern and biochemical properties of the R235E mutant closely resemble those of I164D, most likely this mutation only influences the NBD-SBD α contacts, not the NBD-SBD β contacts. Taken together, the NBD-SBD β contacts are more resistant to disruptions than the NBD-SBD α contacts. This is consistent with the reported SAXS studies (59).

For DnaK, the most studied Hsp70, it was reported that a minimal affinity of 7 μ M for peptide substrates is needed to trigger a stimulation of the intrinsic ATPase activity (76). Although the affinities of Msi3 for both the TRP2_181 and TRP2-Bpa peptides are higher than 7 μ M (Fig. 4, C and D, and S5A), little stimulation of the cryptic ATPase activity was observed even after stabilization with cross-linking. It is possible that Hsp70s and Hsp110s have important differences in binding peptide substrates. Indeed, they prefer different peptide substrates (58, 61). In addition, their intrinsic ATPase activities are different: Hsp70s alone have an intrinsic ATPase activity, whereas there is little ATPase for Hsp110s by themselves.

An interesting feature about Hsp110s and Hsp70s is their essential but different roles in presenting tumor antigens (64). Hsp70s mainly present peptides as tumor antigens. In contrast, Hsp110s prefer to present large proteins such as Her2 as tumor antigen, suggesting that Hsp110s may prefer large protein substrates. Consistent with this, denatured luciferase has been shown to increase the ATPase activity of Hsp110 (20) although we observed little stimulation on the ATPase of Msi3 by denatured luciferase in our preliminary studies (data not shown). Different from peptide substrates, large protein substrates may have various partially folded structures and provide multiple binding sites. Thus, large protein substrates may show an enhanced affinity for Hsp110s, which may be able to trigger the interdomain coupling that is necessary to release the suppression of the cryptic ATPase activity and then stimulate the ATPase activity of Hsp110s.

Another interesting observation from this study is the different effects of the peptide substrates on the formation of the Msi3-Ssa1 complex. The NR peptide comigrated with the Msi3-Ssa1 complex, most likely through binding to Ssa1; whereas after cross-linked to the TRP2-Bpa peptide, Msi3 failed to form stable complexes with Ssa1. Thus, a triple complex among Msi3, Ssa1, and a polypeptide substrate can form stably when Ssa1 binds polypeptide substrates. Hsp70s bind polypeptide substrates stably, whereas Hsp110s seem to bind peptide substrates only transiently on their own. It is possible that Hsp70 first binds polypeptide substrates. Then, through its interaction with Hsp110, Hsp70 may bring the substrates to Hsp110. Thus, Hsp110 and Hsp70 could bind to

the same polypeptide substrate at different segments. This may stabilize the transient Hsp110–substrate binding.

It has been proposed that Hsp110s coordinate with Hsp70s in actively binding and releasing polypeptide substrates during the chaperone cycle (4, 56, 58, 61). It is clear that Hsp110 forms a stable complex with Hsp70 in this process. An important question is when this Hsp70–Hsp110 complex dissociates during the functional chaperone cycle. Dissociation of this essential complex must be an important step of a productive chaperone cycle. Although a previous study showed that ATP binding to Ssa1 can reduce the Sse1–Ssa1 complex, there was still a significant amount of the complex in the presence of a large amount of ATP, suggesting that the dissociation of the Sse1–Ssa1 complex by ATP binding to Ssa1 is not efficient (22). This is consistent with many studies on the complex formation including our native gel analysis (22, 56, 80). The complex is quite stable in the presence of a large amount of ATP in our native gel analysis. Thus, ATP binding to Hsp70s may be a factor for dissociating the Hsp110–Hsp70 complex, but it does not seem to be the definitive factor. Studies suggest that the ATP-bound conformation of Hsp110s is essential for forming and maintaining the Hsp110–Hsp70 complex (22, 56). Regulating the ATP-bound state of Hsp110 seems to be a more efficient approach for regulating the complex formation and dissociation than alternatives. Our study provides support for this hypothesis. Stable peptide substrate binding prevented Msi3 from forming a stable complex with Ssa1 through disrupting the ATP-bound state of Msi3. In addition, our preliminary studies suggested that even after the Msi3–Ssa1 complex was first formed, cross-linking the TRP2–Bpa peptide also significantly reduced the amount of the complex formation between Msi3 and Ssa1 (data not shown). Thus, forming a stable complex with peptide substrates for Msi3 may be one of the major triggers for dissociating the Hsp110–Hsp70 complex.

Experimental Procedures

Protein expression and purification

All the Msi3 and Sse1 proteins used in this study were expressed using the pSMT3 plasmid and purified as described previously with some modifications (40, 71). The pSMT3 plasmid was a generous gift from Dr Christopher Lima (Sloan Kettering Institute) (89). Briefly, the *MSI3* ORF was amplified using PCR from the genomic DNA of the yeast *C. albicans* (generously provided by Dr Ronda Rolfes, Georgetown University) and inserted into the pSMT3 vector through the BamHI and XhoI cloning sites to express as a Smt3–Msi3 fusion protein. The mutations were introduced into the pSMT3–*MSI3* plasmids using mutagenic PCR. All the Msi3 proteins were expressed in Rosetta2(DE3)pLysS strain (MilliporeSigma Novagen) and the Sse1 protein was expressed in BL21(DE3). The induction of expression was carried out at 18 °C for about 8 h for all the proteins to ensure proper folding. The expressed His6–Smt3–Msi3 and His6–Smt3–Sse1 fusion proteins were first purified on a HisTrap column (GE Healthcare Life Sciences) using 25 mM Hepes–NaOH, pH 7.5,

as buffer. To remove any contaminations of the endogenous chaperones from *E. coli* such as DnaK, the Ni column was washed extensively with a buffer containing 200 μM ATP. The His6–Smt3 tag was cleaved by Ulp1 protease and removed by a second HisTrap column. To remove any ATP bound to the Msi3 and Sse1 proteins, an extensive dialysis using a buffer containing 5 mM EDTA was carried out. After further purified on a HiTrap Q column, the peak fractions were concentrated to >10 mg/ml in buffer containing 25 mM Hepes–KOH, pH 7.5, 50 mM KCl, and 1 mM DTT, flash frozen in liquid nitrogen, and stored in –80 °C freezers.

The Ssa1 protein was purified from the yeast *Pichia pastoris*, and the Ssa1-expressing *Pichia* strain was a generous gift from Dr Johannes Buchner (Technische Universität München) (90). The induction and purification process were based on the published method with some modifications (79, 90). Briefly, an overnight culture was grown in YPD supplemented with Zeocin (100 μg/ml) at 30 °C and pelleted by centrifugation at 5000g. The pellet was resuspended in YP medium containing 0.5% methanol and grown at 30 °C for 24 h to induce expression of Ssa1. After induction, the cell lysate was prepared using EmulsiFlex–C3 homogenizer. After centrifugation to remove cell debris, the lysate was first purified on a HiTrap Q column using buffers containing 25 mM Hepes–NaOH, pH 7.5, and 1 mM EDTA. The fractions containing Ssa1 were dialyzed and incubated with 5–10 ml ATP–agarose resin (Sigma–Aldrich) for one overnight. After extensive washing, the Ssa1 protein was eluted with ATP from the ATP–agarose resin. The Ssa1 protein was further purified on a HiTrap Q column after dialyzed in a buffer containing 2 mM EDTA to remove ATP. Before flash frozen in liquid nitrogen, the purified Ssa1 was concentrated to >10 mg/ml.

The Ydj1 and Sis1 proteins were expressed and purified in a similar way as the Sse1 proteins. Briefly, the ORFs of Ydj1 and Sis1 were inserted into the pSMT3 plasmid and expressed as a Smt3 fusion protein with a His6 tag at the N-terminus in BL21(DE3) at 30 °C. The fusion proteins were first purified on a HisTrap column. After cleavage of the His6–Smt3 tag using Ulp1 protease, the Ydj1 and Sis1 proteins were further purified on HiTrap Q and S column, respectively, after going through a second Ni column to remove the cleaved tag. The firefly luciferase was cloned, expressed, and purified in a similar way as that of Msi3. All the purified proteins were concentrated to >10 mg/ml, flash frozen in liquid nitrogen, and stored in –80 °C freezers.

Site-directed mutagenesis, growth tests in yeast, and Western blot analysis of the Msi3 expression level

Mutagenesis in Msi3 and growth tests of Msi3 mutations in yeast *S. cerevisiae* were carried out as described before for Sse1 (40, 71). Briefly, the *MSI3* ORF was inserted into the yeast vector pRS313 with the endogenous promoter of Sse1 right in front of the *MSI3* ORF. Thus, the resulting plasmid, pRS313–*MSI3*, has the WT *MSI3* gene under the control of the Sse1 promoter. The Msi3 mutations were introduced into the pRS313–*MSI3* plasmid using the site-directed mutagenesis

The unique allosteric regulation of Hsp110

with mutagenic primers. After transforming into a *SSE1* deletion strain, *YPL106C BY4742 (MAT α his3 Δ 1 leu2 Δ 0 lys2 Δ 0 ura3 Δ 0 trp1 Δ 1 Δ SSE1)*, fresh transformants were dropped onto agar plates containing yeast minimum media lacking histidine. Growth tests were carried out with incubation at 37 °C for 3–4 days with a control growth done at 30 °C.

The expression levels of Msi3 mutants in yeast were assayed using Western blotting analysis with an anti-Sse1 antibody as described previously (40). This antibody recognizes Msi3 due to the high sequence identity between Msi3 and Sse1. Briefly, fresh overnight cultures grown at 30 °C were shifted to 37 °C for 2 h. Then, 2 O.D. of each culture was harvested and resuspended in 50 μ l PBS buffer (16 mM Na₂HPO₄, 4 mM NaH₂PO₄, 150 mM NaCl and 1 mM PMSF). After adding 60 μ l SDS-Triton (2% SDS and 0.2% Triton X-100), ~30 μ l acid-washed glass beads were added and a 2-min vortex was applied to break open yeast. After centrifugation, the cell lysates were loaded on a SDS-PAGE and Western blotting analysis was carried out. All growth tests and the corresponding Western blotting analysis were repeated more than three times with at least two independent transformations.

Luciferase refolding assay using Ssa1, Msi3, and Ydj1

The assay was carried out in a similar way as in the previous publications with modifications (4, 56, 71). Briefly, purified firefly luciferase was diluted with buffer A (25 mM Hepes-KOH, pH 7.5, 100 mM KCl, 10 mM Mg(OAc)₂, 1 mM DTT, and 3 mM ATP). The final concentration of luciferase was 110 nM and 30 μ M Ssa1 was included in this dilution. The luciferase was denatured by incubating at 42 °C for 15 min. Refolding reactions were started by diluting the denatured luciferase into a reaction mixture containing 30 μ M Ssa1, 4 μ M Ydj1, and 2 μ M Msi3 in buffer A. After incubating at room temperature for 10, 20, and 30 min, the luciferase activities were measured in a luminometer (Berthold LB9507) by mixing 2 μ l of refolding reactions with 50 μ l of luciferase substrate (Promega). Relative luciferase activities were calculated by setting the activity of the unheated luciferase as 100%. All the biochemical assays were repeated more than three times with at least two different protein purifications. All the data points were input into PRISM (GraphPad). Then mean and SD were calculated and plotted as a function of reaction time.

Limited trypsin digest for conformational tests

The assay was carried out essentially the same way as published before on Sse1 (40, 71). Briefly, Msi3 proteins were diluted to 1 mg/ml using buffer B (25 mM Hepes-KOH, pH 7.5, 150 mM KCl, 10 mM Mg(OAc)₂, 10% glycerol, and 1 mM DTT). An equal volume of trypsin (20 μ g/ml) was mixed with Msi3 protein in the presence or absence of 2 mM ATP. The reaction was incubated at 25 °C for 30 min. After adding PMSF to a final concentration of 1 mM to stop the trypsin digest reactions, aliquots were loaded on to 15% SDS-PAGE gels and visualized with Coomassie staining. The assay was repeated more than three times for every protein with at least

two independent purifications. Representative gels were shown.

Single-turnover ATPase assay

The assay was performed as described previously for Hsp70s (58, 91). First, 20 μ g of Msi3 protein was incubated with 25 μ Ci of [α -³²P]ATP (NEG503H250UC, 3000 Ci/mmol; PerkinElmer Life Sciences) in 100 μ l buffer C (25 mM Hepes-KOH, pH 7.5, 100 mM KCl, 10 mM Mg(OAc)₂, 1 mM DTT, 10% glycerol) in the presence of 20 μ M unlabeled ATP on ice for 5 min to allow a complex between Msi3 and ATP to form. Then, the Msi3-ATP complex was quickly isolated from free ATP using a spin column at 4 °C. To start the ATPase assay, the Msi3-ATP complex was mixed with an equal volume of buffer A and incubated at 25 °C. At the indicated time points, aliquots of the ATPase reactions were taken and stopped by adding 1 M formic acid, 0.5 M LiCl, and 250 μ M ATP. ATP and ADP were separated on a polyethyleneimine-cellulose thin-layer chromatography plates and quantified after being visualized using a Typhoon phosphorimaging system (GE Healthcare). The percentage of ATP hydrolysis was calculated as ADP/(ADP + ATP). Mean and SD were calculated after each data point for ATP hydrolysis was input into PRISM (GraphPad). The data was plotted as a function of reaction time. After fitting the data using the first-order rate equation, the rates of ATP hydrolysis (k_{cat}) were deduced.

Fluorescence polarization assay for ATP binding

To determine the ATP-binding affinity, a fluorescence polarization assay was carried out as described previously (71, 88). A fluorescence-labeled ATP, N6-(6-amino)hexyl-ATP-5-FAM (ATP-FAM) (Jena Bioscience), was used. Serial dilutions of Msi3 proteins were prepared and incubated with ATP-FAM (a final concentration of 20 nM) in buffer B for 1 h at room temperature to allow binding to reach equilibrium. Then, fluorescence polarization was measured using a Beacon 2000 instrument (Invitrogen). The fluorescence polarization values were expressed in millipolarization (mP) units. Using GraphPad Prism software, the binding data were fitted to a one-site binding equation to calculate dissociation constants (K_d).

Fluorescence anisotropy assays for peptide substrate-binding affinity

The TRP2, TRP2-Bpa, and NR peptides were labeled with fluorescein at the N terminus and ordered from NEO-Bioscience (at > 95% purity). Binding affinity assays using fluorescence polarization were carried out as described previously with some modifications (58). Briefly, serial dilutions of Msi3 proteins were prepared in buffer B and incubated with peptides at a final concentration of 10 nM. For the assays in the presence of ADP or ATP, 50 μ M ADP or 2 mM ATP was included. After the binding reached equilibrium, fluorescence polarization measurements were carried out on Beacon 2000 (Invitrogen) and dissociation constants (K_d) were calculated using PRISM (GraphPad).

Preventing aggregation assay

We used the purified firefly luciferase as a model substrate to analyze the preventing aggregation activity of Msi3. The assay was performed in a similar way as described previously for Sse1 and Msi3 (19, 58, 71). The luciferase was diluted with buffer D (25 mM Hepes-KOH, pH 7.5, 150 mM KCl, 10 mM Mg(OAc)₂, and 1 mM DTT) in the presence of Msi3. The final concentrations of luciferase and Msi3 were 750 nM and 3 μM, respectively. The aggregation of luciferase was induced by an incubation at 42 °C. UV absorbance at 320 nm was used to monitor protein aggregation. Luciferase or Msi3 alone was used as a control. For the reactions in the presence of ATP or ADP, ATP and ADP were added to a final concentration of 3 mM and 200 μM, respectively. Each data point was input into PRISM (GraphPad), using which mean and SD were calculated. The data was plotted as a function of reaction time using PRISM.

The NEF activity assay

The assay was performed in a similar way as described recently (71, 88). First, a complex of Ssa1 and ATP-FAM was formed by incubating 1 μM Ssa1 with 20 nM ATP-FAM in buffer B for 1 h on ice. Then, this complex was rapidly mixed with 1 μM Msi3 protein in the presence or absence of 50 μM of ATP at 25 °C and the decreases in fluorescent polarization over time were recorded on a Beacon 2000 instrument (Invitrogen). 50 μM ATP alone was used as a control.

UV cross-linking of the TRP2-Bpa peptide to the Msi3 and Ssa1 proteins

The cross-linking was carried out as described previously (79). Briefly, the Msi3 and Ssa1 proteins were diluted to 14 μM using buffer B. For the proteins used in the ATPase assay, limited trypsin digest analysis, and native gel analysis, the ratio of protein to the TRP2-Bpa peptide is 1:8 and the UV treatment is 30 min on ice. For testing the ratios of the protein to the TRP2-Bpa peptide, UV treatment on ice for 60 min was used to enhance cross-linking.

Native gel analysis for protein-peptide and protein-protein complexes

The Msi3 and Ssa1 proteins and the peptides were diluted using buffer B. When forming Msi3-Ssa1 complex, the Msi3 (10 μM) and Ssa1 (12 μM) proteins were mixed together with a final concentration of ATP at 4 mM and incubated on ice for 20 min. For the samples with peptides, the NR or TRP2-Bpa peptide was included at 1:8 M ratio (protein over peptide). The samples were applied to 10% native gels (run at 140 V for 1.5 h on ice). The peptides were visualized with a Typhoon phosphorimaging system (GE Healthcare) since they were labeled with fluorescein. Afterward, the proteins were stained with Coomassie Blue. Each native gel and corresponding SDS gel were repeated more than three times using freshly prepared protein samples from at least two different purifications.

Data availability

All the data described in the manuscript are contained within the manuscript.

Supporting information—This article contains [supporting information](#).

Acknowledgments—We thank Drs Jiao Yang, Cancan Sun, and Srinivas Sistla, Baoxiu Zhang, Huanyu Zhu, Ying Wang, Ce Liang, Jiayue Su, and Jessica Ramirez for technical support and discussion. We thank Drs Xianjun Fang and Wei Wang for helping us with Western blot analysis.

Author contributions—H. L., Qingdai Liu, L. Z., and Qinglian Liu conceptualization; H. L., L. H., C. W. C., Qianbin Li, Qingdai Liu, L. Z., and Qinglian Liu data curation; H. L., L. H., Qingdai Liu, L. Z., and Qinglian Liu formal analysis; Qinglian Liu funding acquisition; H. L. and L. H. investigation; H. L., L. H., M. M., Qingdai Liu, L. Z., and Qinglian Liu methodology; Qinglian Liu project administration; Qinglian Liu resources; H. L., Qianbin Li, Qingdai Liu, L. Z., and Qinglian Liu supervision; H. L. and Qinglian Liu validation; H. L., L. H., Qingdai Liu, L. Z., and Qinglian Liu visualization; H. L., Qingdai Liu, L. Z., and Qinglian Liu writing—original draft; H. L., L. H., C. W. C., M. M., Qianbin Li, Qingdai Liu, L. Z., and Qinglian Liu writing—review and editing.

Funding and additional information—This work was supported by NIH (R01GM098592 and R21AI140006 to Qinglian Liu) and VETAR award from the Virginia Commonwealth University (to Qinglian Liu). L. Z. was partially supported by R01GM109193 from NIH. The content is solely the responsibility of the authors and does not necessarily represent the official views of the National Institutes of Health.

Conflict of interest—The authors declare that they have no conflicts of interest with the contents of this article.

Abbreviations—The abbreviations used are: Hsp110, Heat shock protein 110 kDa; Hsp70, heat shock protein 70 kDa; NEF, nucleotide-exchange factor; NBD, nucleotide-binding domain; SBD, substrate-binding domain; ATP, adenosine triphosphate; ATPase, adenosine triphosphatase; ADP, adenosine diphosphate; Sse1, stress seventy E1; Msi3, a multicopy suppressor of the heat shock-sensitive phenotype of the viral mutation.

References

1. Easton, D. P., Kaneko, Y., and Subject, J. R. (2000) The hsp110 and Grp170 stress proteins: Newly recognized relatives of the Hsp70s. *Cell Stress Chaperones* 5, 276–290
2. Lee-Yoon, D., Easton, D., Murawski, M., Burd, R., and Subject, J. R. (1995) Identification of a major subfamily of large hsp70-like proteins through the cloning of the mammalian 110-kDa heat shock protein. *J. Biol. Chem.* 270, 15725–15733
3. Raviol, H., Sadlish, H., Rodriguez, F., Mayer, M. P., and Bukau, B. (2006) Chaperone network in the yeast cytosol: Hsp110 is revealed as an Hsp70 nucleotide exchange factor. *EMBO J.* 25, 2510–2518
4. Dragovic, Z., Broadley, S. A., Shomura, Y., Bracher, A., and Hartl, F. U. (2006) Molecular chaperones of the Hsp110 family act as nucleotide exchange factors of Hsp70s. *EMBO J.* 25, 2519–2528
5. Yam, A. Y., Albanese, V., Lin, H. T., and Frydman, J. (2005) Hsp110 cooperates with different cytosolic HSP70 systems in a pathway for de novo folding. *J. Biol. Chem.* 280, 41252–41261

The unique allosteric regulation of Hsp110

- Shaner, L., Trott, A., Goeckeler, J. L., Brodsky, J. L., and Morano, K. A. (2004) The function of the yeast molecular chaperone Sse1 is mechanistically distinct from the closely related hsp70 family. *J. Biol. Chem.* **279**, 21992–22001
- Liu, X. D., Morano, K. A., and Thiele, D. J. (1999) The yeast Hsp110 family member, Sse1, is an Hsp90 cochaperone. *J. Biol. Chem.* **274**, 26654–26660
- Shaner, L., and Morano, K. A. (2007) All in the family: Atypical Hsp70 chaperones are conserved modulators of Hsp70 activity. *Cell Stress Chaperones* **12**, 1–8
- Yakubu, U. M., and Morano, K. A. (2018) Roles of the nucleotide exchange factor and chaperone Hsp110 in cellular proteostasis and diseases of protein misfolding. *Biol. Chem.* **399**, 1215–1221
- Bukau, B., Weissman, J., and Horwich, A. (2006) Molecular chaperones and protein quality control. *Cell* **125**, 443–451
- Mayer, M. P., and Bukau, B. (2005) Hsp70 chaperones: Cellular functions and molecular mechanism. *Cell Mol. Life Sci.* **62**, 670–684
- Balchin, D., Hayer-Hartl, M., and Hartl, F. U. (2016) *In vivo* aspects of protein folding and quality control. *Science* **353**, aac4354
- Young, J. C. (2010) Mechanisms of the Hsp70 chaperone system. *Biochem. Cell Biol.* **88**, 291–300
- Liu, Q., Liang, C., and Zhou, L. (2020) Structural and functional analysis of the Hsp70/Hsp40 chaperone system. *Protein Sci.* **29**, 378–390
- Fernandez-Fernandez, M. R., and Valpuesta, J. M. (2018) Hsp70 chaperone: A master player in protein homeostasis. *F1000Res* **7**, F1000 Faculty Rev-1497
- Pobre, K. F. R., Poet, G. J., and Hendershot, L. M. (2019) The endoplasmic reticulum (ER) chaperone BiP is a master regulator of ER functions: Getting by with a little help from ERdj friends. *J. Biol. Chem.* **294**, 2098–2108
- Zuiderweg, E. R., Hightower, L. E., and Gestwicki, J. E. (2017) The remarkable multivalency of the Hsp70 chaperones. *Cell Stress Chaperones* **22**, 173–189
- Oh, H. J., Chen, X., and Subjeck, J. R. (1997) Hsp110 protects heat-denatured proteins and confers cellular thermoresistance. *J. Biol. Chem.* **272**, 31636–31640
- Goeckeler, J. L., Stephens, A., Lee, P., Caplan, A. J., and Brodsky, J. L. (2002) Overexpression of yeast Hsp110 homolog Sse1p suppresses ydj1-151 thermosensitivity and restores Hsp90-dependent activity. *Mol. Biol. Cell* **13**, 2760–2770
- Mattoo, R. U., Sharma, S. K., Priya, S., Finka, A., and Goloubinoff, P. (2013) Hsp110 is a bona fide chaperone using ATP to unfold stable misfolded polypeptides and reciprocally collaborate with Hsp70 to solubilize protein aggregates. *J. Biol. Chem.* **288**, 21399–21411
- Taguchi, Y. V., Gorenberg, E. L., Nagy, M., Thrasher, D., Fenton, W. A., Volpicelli-Daley, L., Horwich, A. L., and Chandra, S. S. (2019) Hsp110 mitigates alpha-synuclein pathology *in vivo*. *Proc. Natl. Acad. Sci. U. S. A.* **116**, 24310–24316
- Andreasson, C., Fiaux, J., Rampelt, H., Mayer, M. P., and Bukau, B. (2008) Hsp110 is a nucleotide-activated exchange factor for Hsp70. *J. Biol. Chem.* **283**, 8877–8884
- Bracher, A., and Verghese, J. (2015) The nucleotide exchange factors of Hsp70 molecular chaperones. *Front. Mol. Biosci.* **2**, 10
- Shaner, L., Wegele, H., Buchner, J., and Morano, K. A. (2005) The yeast Hsp110 Sse1 functionally interacts with the Hsp70 chaperones Ssa and Ssb. *J. Biol. Chem.* **280**, 41262–41269
- Albanese, V., Yam, A. Y., Baughman, J., Parnot, C., and Frydman, J. (2006) Systems analyses reveal two chaperone networks with distinct functions in eukaryotic cells. *Cell* **124**, 75–88
- Fan, Q., Park, K. W., Du, Z., Morano, K. A., and Li, L. (2007) The role of Sse1 in the de novo formation and variant determination of the [PSI⁺] prion. *Genetics* **177**, 1583–1593
- Hrizo, S. L., Gusarova, V., Habel, D. M., Goeckeler, J. L., Fisher, E. A., and Brodsky, J. L. (2007) The Hsp110 molecular chaperone stabilizes apolipoprotein B from endoplasmic reticulum-associated degradation (ERAD). *J. Biol. Chem.* **282**, 32665–32675
- Shorter, J. (2011) The mammalian disaggregase machinery: Hsp110 synergizes with Hsp70 and Hsp40 to catalyze protein disaggregation and reactivation in a cell-free system. *PLoS One* **6**, e26319
- Torrente, M. P., and Shorter, J. (2013) The metazoan protein disaggregase and amyloid depolymerase system: Hsp110, Hsp70, Hsp40, and small heat shock proteins. *Prion* **7**, 457–463
- Muralidharan, V., Oksman, A., Pal, P., Lindquist, S., and Goldberg, D. E. (2012) Plasmodium falciparum heat shock protein 110 stabilizes the asparagine repeat-rich parasite proteome during malarial fevers. *Nat. Commun.* **3**, 1310
- Rampelt, H., Kirstein-Miles, J., Nillegoda, N. B., Chi, K., Scholz, S. R., Morimoto, R. I., and Bukau, B. (2012) Metazoan Hsp70 machines use Hsp110 to power protein disaggregation. *EMBO J.* **31**, 4221–4235
- Mandal, A. K., Gibney, P. A., Nillegoda, N. B., Theodoraki, M. A., Caplan, A. J., and Morano, K. A. (2010) Hsp110 chaperones control client fate determination in the hsp70-Hsp90 chaperone system. *Mol. Biol. Cell* **21**, 1439–1448
- Ravindran, M. S., Bagchi, P., Inoue, T., and Tsai, B. (2015) A non-enveloped virus hijacks host disaggregation machinery to translocate across the endoplasmic reticulum membrane. *PLoS Pathog.* **11**, e1005086
- Gao, X., Carroni, M., Nussbaum-Krammer, C., Mogk, A., Nillegoda, N. B., Szlachcic, A., Guilbride, D. L., Saibil, H. R., Mayer, M. P., and Bukau, B. (2015) Human Hsp70 disaggregase reverses Parkinson's-linked alpha-synuclein amyloid fibrils. *Mol. Cell* **59**, 781–793
- Kandasamy, G., and Andreasson, C. (2018) Hsp70-Hsp110 chaperones deliver ubiquitin-dependent and -independent substrates to the 26S proteasome for proteolysis in yeast. *J. Cell Sci.* **131**, jcs210948
- Moran, C., Kinsella, G. K., Zhang, Z. R., Perrett, S., and Jones, G. W. (2013) Mutational analysis of Sse1 (Hsp110) suggests an integral role for this chaperone in yeast prion propagation *in vivo*. *G3 (Bethesda)* **3**, 1409–1418
- O'Driscoll, J., Clare, D., and Saibil, H. (2015) Prion aggregate structure in yeast cells is determined by the Hsp104-Hsp110 disaggregase machinery. *J. Cell Biol.* **211**, 145–158
- Hatayama, T., and Yasuda, K. (1998) Association of HSP105 with HSC70 in high molecular mass complexes in mouse FM3A cells. *Biochem. Biophys. Res. Commun.* **248**, 395–401
- Wang, X. Y., Chen, X., Oh, H. J., Repasky, E., Kazim, L., and Subjeck, J. (2000) Characterization of native interaction of hsp110 with hsp25 and hsc70. *FEBS Lett.* **465**, 98–102
- Liu, Q., and Hendrickson, W. A. (2007) Insights into Hsp70 chaperone activity from a crystal structure of the yeast Hsp110 Sse1. *Cell* **131**, 106–120
- Yakubu, U. M., and Morano, K. A. (2021) Suppression of aggregate and amyloid formation by a novel intrinsically disordered region in metazoan Hsp110 chaperones. *J. Biol. Chem.*, 100567
- Oh, H. J., Easton, D., Murawski, M., Kaneko, Y., and Subjeck, J. R. (1999) The chaperoning activity of hsp110. Identification of functional domains by use of targeted deletions. *J. Biol. Chem.* **274**, 15712–15718
- Mayer, M. P., and Gierasch, L. M. (2019) Recent advances in the structural and mechanistic aspects of Hsp70 molecular chaperones. *J. Biol. Chem.* **294**, 2085–2097
- Bukau, B., and Horwich, A. L. (1998) The Hsp70 and Hsp60 chaperone machines. *Cell* **92**, 351–366
- Buchberger, A., Theyssen, H., Schroder, H., McCarty, J. S., Virgallita, G., Milkereit, P., Reinstein, J., and Bukau, B. (1995) Nucleotide-induced conformational changes in the ATPase and substrate binding domains of the DnaK chaperone provide evidence for interdomain communication. *J. Biol. Chem.* **270**, 16903–16910
- Swain, J. F., Dinler, G., Sivendran, R., Montgomery, D. L., Stotz, M., and Gierasch, L. M. (2007) Hsp70 chaperone ligands control domain association via an allosteric mechanism mediated by the interdomain linker. *Mol. Cell* **26**, 27–39
- Bertelsen, E. B., Chang, L., Gestwicki, J. E., and Zuiderweg, E. R. (2009) Solution conformation of wild-type E. coli Hsp70 (DnaK) chaperone complexed with ADP and substrate. *Proc. Natl. Acad. Sci. U. S. A.* **106**, 8471–8476
- Schmid, D., Baici, A., Gehring, H., and Christen, P. (1994) Kinetics of molecular chaperone action. *Science* **263**, 971–973
- Flynn, G. C., Chappell, T. G., and Rothman, J. E. (1989) Peptide binding and release by proteins implicated as catalysts of protein assembly. *Science* **245**, 385–390

50. Kityk, R., Kopp, J., Sinning, I., and Mayer, M. P. (2012) Structure and dynamics of the ATP-bound open conformation of Hsp70 chaperones. *Mol. Cell* **48**, 863–874
51. Qi, R., Sarbeng, E. B., Liu, Q., Le, K. Q., Xu, X., Xu, H., Yang, J., Wong, J. L., Vorvis, C., Hendrickson, W. A., and Zhou, L. (2013) Allosteric opening of the polypeptide-binding site when an Hsp70 binds ATP. *Nat. Struct. Mol. Biol.* **20**, 900–907
52. Yang, J., Zong, Y., Su, J., Li, H., Zhu, H., Columbus, L., Zhou, L., and Liu, Q. (2017) Conformation transitions of the polypeptide-binding pocket support an active substrate release from Hsp70s. *Nat. Commun.* **8**, 1201
53. Zhuravleva, A., and Gierasch, L. M. (2011) Allosteric signal transmission in the nucleotide-binding domain of 70-kDa heat shock protein (Hsp70) molecular chaperones. *Proc. Natl. Acad. Sci. U. S. A.* **108**, 6987–6992
54. Alderson, T. R., Kim, J. H., and Markley, J. L. (2016) Dynamical structures of Hsp70 and Hsp70-Hsp40 complexes. *Structure* **24**, 1014–1030
55. Gumiero, A., Conz, C., Gese, G. V., Zhang, Y., Weyer, F. A., Lapouge, K., Kappes, J., von Plehwe, U., Schermann, G., Fitzke, E., Wolffe, T., Fischer, T., Rospert, S., and Sinning, I. (2016) Interaction of the cotranslational Hsp70 Ssb with ribosomal proteins and rRNA depends on its lid domain. *Nat. Commun.* **7**, 13563
56. Polier, S., Dragovic, Z., Hartl, F. U., and Bracher, A. (2008) Structural basis for the cooperation of Hsp70 and Hsp110 chaperones in protein folding. *Cell* **133**, 1068–1079
57. Yamagishi, N., Ishihara, K., and Hatayama, T. (2004) Hsp105alpha suppresses Hsc70 chaperone activity by inhibiting Hsc70 ATPase activity. *J. Biol. Chem.* **279**, 41727–41733
58. Xu, X., Sarbeng, E. B., Vorvis, C., Kumar, D. P., Zhou, L., and Liu, Q. (2012) The unique peptide substrate binding properties of 110 KDA heatshock protein (HSP110) determines its distinct chaperone activity. *J. Biol. Chem.* **287**, 5661–5672
59. Kumar, V., Peter, J. J., Sagar, A., Ray, A., Jha, M. P., Rebeaud, M. E., Tiwari, S., Goloubinoff, P., Ashish, F., and Mapa, K. (2020) Inter-domain communication suppressing high intrinsic ATPase activity of Sse1 is essential for its co-disaggregase activity with Ssa1. *FEBS J.* **287**, 671–694
60. Raviol, H., Bukau, B., and Mayer, M. P. (2006) Human and yeast Hsp110 chaperones exhibit functional differences. *FEBS Lett.* **580**, 168–174
61. Goeckeler, J. L., Petruso, A. P., Aguirre, J., Clement, C. C., Chiosis, G., and Brodsky, J. L. (2008) The yeast Hsp110, Sse1p, exhibits high-affinity peptide binding. *FEBS Lett.* **582**, 2393–2396
62. Manjili, M. H., Henderson, R., Wang, X. Y., Chen, X., Li, Y., Repasky, E., Kazim, L., and Subjeck, J. R. (2002) Development of a recombinant HSP110-HER-2/neu vaccine using the chaperoning properties of HSP110. *Cancer Res.* **62**, 1737–1742
63. Xu, X., Sarbeng, E. B., Vorvis, C., Kumar, D. P., Zhou, L., and Liu, Q. (2012) Unique peptide substrate binding properties of 110-kDa heat-shock protein (Hsp110) determine its distinct chaperone activity. *J. Biol. Chem.* **287**, 5661–5672
64. Zuo, D., Subjeck, J., and Wang, X. Y. (2016) Unfolding the role of large heat shock proteins: New insights and therapeutic implications. *Front. Immunol.* **7**, 75
65. Mukai, H., Kuno, T., Tanaka, H., Hirata, D., Miyakawa, T., and Tanaka, C. (1993) Isolation and characterization of SSE1 and SSE2, new members of the yeast HSP70 multigene family. *Gene* **132**, 57–66
66. Schuermann, J. P., Jiang, J., Cuellar, J., Llorca, O., Wang, L., Gimenez, L. E., Jin, S., Taylor, A. B., Demeler, B., Morano, K. A., Hart, P. J., Valpuesta, J. M., Lafer, E. M., and Sousa, R. (2008) Structure of the Hsp110:Hsc70 nucleotide exchange machine. *Mol. Cell* **31**, 232–243
67. Hendrickson, W. A., and Liu, Q. (2008) Exchange we can believe in. *Structure* **16**, 1153–1155
68. Andreasson, C., Fiaux, J., Rampelt, H., Druffel-Augustin, S., and Bukau, B. (2008) Insights into the structural dynamics of the Hsp110-Hsp70 interaction reveal the mechanism for nucleotide exchange activity. *Proc. Natl. Acad. Sci. U. S. A.* **105**, 16519–16524
69. Nagao, J., Cho, T., Uno, J., Ueno, K., Imayoshi, R., Nakayama, H., Chibana, H., and Kaminishi, H. (2012) Candida albicans Msi3p, a homolog of the Saccharomyces cerevisiae Sse1p of the Hsp70 family, is involved in cell growth and fluconazole tolerance. *FEMS Yeast Res.* **12**, 728–737
70. Cho, T., Toyoda, M., Sudoh, M., Nakashima, Y., Calderone, R. A., and Kaminishi, H. (2003) Isolation and sequencing of the Candida albicans MSI3, a putative novel member of the HSP70 family. *Yeast* **20**, 149–156
71. Wang, Y., Li, H., Sun, C., Liu, Q., Zhou, L., and Liu, Q. (2021) Purification and biochemical characterization of Msi3, an essential Hsp110 molecular chaperone in Candida albicans. *Cell Stress Chaperones* **26**, 695–704
72. Flaherty, K. M., DeLuca-Flaherty, C., and McKay, D. B. (1990) Three-dimensional structure of the ATPase fragment of a 70K heat-shock cognate protein. *Nature* **346**, 623–628
73. Sriram, M., Osipiuk, J., Freeman, B., Morimoto, R., and Joachimiak, A. (1997) Human Hsp70 molecular chaperone binds two calcium ions within the ATPase domain. *Structure* **5**, 403–414
74. Yang, J., Nune, M., Zong, Y., Zhou, L., and Liu, Q. (2015) Close and allosteric opening of the polypeptide-binding site in a human Hsp70 chaperone BiP. *Structure* **23**, 2191–2203
75. Gozzi, G. J., Gonzalez, D., Boudesco, C., Dias, A. M. M., Gotthard, G., Uyanik, B., Dondaine, L., Marcino, G., Hermetet, F., Denis, C., Hardy, L., Suzanne, P., Douhard, R., Jego, G., Dubrez, L., et al. (2020) Selecting the first chemical molecule inhibitor of HSP110 for colorectal cancer therapy. *Cell Death Differ.* **27**, 117–129
76. Mayer, M. P., Schroder, H., Rudiger, S., Paal, K., Laufen, T., and Bukau, B. (2000) Multistep mechanism of substrate binding determines chaperone activity of Hsp70. *Nat. Struct. Biol.* **7**, 586–593
77. Mayer, M. P., Laufen, T., Paal, K., McCarty, J. S., and Bukau, B. (1999) Investigation of the interaction between DnaK and DnaJ by surface plasmon resonance spectroscopy. *J. Mol. Biol.* **289**, 1131–1144
78. Clerico, E. M., Tilitzky, J. M., Meng, W., and Gierasch, L. M. (2015) How hsp70 molecular machines interact with their substrates to mediate diverse physiological functions. *J. Mol. Biol.* **427**, 1575–1588
79. Li, H., Zhu, H., Sarbeng, E. B., Liu, Q., Tian, X., Yang, Y., Lyons, C., Zhou, L., and Liu, Q. (2020) An unexpected second binding site for polypeptide substrates is essential for Hsp70 chaperone activity. *J. Biol. Chem.* **295**, 584–596
80. Shaner, L., Sousa, R., and Morano, K. A. (2006) Characterization of Hsp70 binding and nucleotide exchange by the yeast Hsp110 chaperone Sse1. *Biochemistry* **45**, 15075–15084
81. Nitika, Porter, C. M., Truman, A. W., and Truttmann, M. C. (2020) Post-translational modifications of Hsp70 family proteins: Expanding the chaperone code. *J. Biol. Chem.* **295**, 10689–10708
82. Kaimal, J. M., Kandasamy, G., Gasser, F., and Andreasson, C. (2017) Coordinated Hsp110 and Hsp104 activities power protein disaggregation in Saccharomyces cerevisiae. *Mol. Cell Biol.* **37**, e00027-17
83. Kryndushkin, D., and Wickner, R. B. (2007) Nucleotide exchange factors for Hsp70s are required for [URE3] prion propagation in Saccharomyces cerevisiae. *Mol. Biol. Cell* **18**, 2149–2154
84. Zhu, X., Zhao, X., Burkholder, W. F., Gragerov, A., Ogata, C. M., Gottesman, M. E., and Hendrickson, W. A. (1996) Structural analysis of substrate binding by the molecular chaperone DnaK. *Science* **272**, 1606–1614
85. Gragerov, A., Zeng, L., Zhao, X., Burkholder, W., and Gottesman, M. E. (1994) Specificity of DnaK-peptide binding. *J. Mol. Biol.* **235**, 848–854
86. Rudiger, S., Germeroth, L., Schneider-Mergener, J., and Bukau, B. (1997) Substrate specificity of the DnaK chaperone determined by screening cellulose-bound peptide libraries. *EMBO J.* **16**, 1501–1507
87. Rudiger, S., Buchberger, A., and Bukau, B. (1997) Interaction of Hsp70 chaperones with substrates. *Nat. Struct. Biol.* **4**, 342–349
88. Garcia, V. M., Nillegoda, N. B., Bukau, B., and Morano, K. A. (2017) Substrate binding by the yeast Hsp110 nucleotide exchange factor and molecular chaperone Sse1 is not obligate for its biological activities. *Mol. Biol. Cell* **28**, 2066–2075

The unique allosteric regulation of Hsp110

89. Mossessova, E., and Lima, C. D. (2000) Ulp1-SUMO crystal structure and genetic analysis reveal conserved interactions and a regulatory element essential for cell growth in yeast. *Mol. Cell* **5**, 865–876
90. Wegele, H., Haslbeck, M., and Buchner, J. (2003) Recombinant expression and purification of Ssa1p (Hsp70) from *Saccharomyces cerevisiae* using *Pichia pastoris*. *J. Chromatogr. B Analyt Technol. Biomed. Life Sci.* **786**, 109–115
91. Davis, J. E., Voisine, C., and Craig, E. A. (1999) Intragenic suppressors of Hsp70 mutants: Interplay between the ATPase- and peptide-binding domains. *Proc. Natl. Acad. Sci. U. S. A.* **96**, 9269–9276